

Robust Representation and Estimation of Barycenters and Modes of Probability Measures on Metric Spaces

Washington Mio and Tom Needham

Abstract

This paper is concerned with the problem of defining and estimating statistics for distributions on spaces such as Riemannian manifolds and more general metric spaces. The challenge comes, in part, from the fact that statistics such as means and modes may be unstable: for example, a small perturbation to a distribution can lead to a large change in Fréchet means on spaces as simple as a circle. We address this issue by introducing a new merge tree representation of barycenters called the barycentric merge tree (BMT), which takes the form of a measured metric graph and summarizes features of the distribution in a multiscale manner. Modes are treated as special cases of barycenters through diffusion distances. In contrast to the properties of classical means and modes, we prove that BMTs are stable—this is quantified as a Lipschitz estimate involving optimal transport metrics. This stability allows us to derive a consistency result for approximating BMTs from empirical measures, with explicit convergence rates. We also give a provably accurate method for discretely approximating the BMT construction and use this to provide numerical examples for distributions on spheres and shape spaces.

Keywords: Fréchet mean, barycenter, median, modes of probability distributions, merge trees.

2020 Mathematics Subject Classification: 62R20, 62R30, 62R40, 55N31

1 Introduction

The core theme of this paper is the development of stable and robust representations for barycenters and modes of probability distributions on metric spaces. The primary goal is to construct simple and provably stable summaries of barycenters and modes for datasets formed of objects that can be of varied nature, so long as they are representable as points in a metric space. This is achieved through a summary representation termed *barycentric merge tree* (BMT).

1.1 Barycenters

The mean of a probability measure μ on Euclidean space \mathbb{R}^d , as the expected value of a random variable $x \in \mathbb{R}^d$ with law μ , has long been used as a simple statistical summary that can be robustly estimated from sufficiently many independent draws from μ . The reinterpretation of the mean as the most central value of x , as measured by variance, dates back at least to É. Cartan in studies of more general forms of centers of mass of distributions on Riemannian manifolds (cf. [6, p. 235]). If μ has finite second moment, the mean is the unique minimizer of the Fréchet variance function $V_2: \mathbb{R}^d \rightarrow \mathbb{R}$ given by

$$V_2(x) := \int_{\mathbb{R}^d} \|y - x\|^2 d\mu(y), \quad (1)$$

the expected value of the squared distance to x [18]. This viewpoint shed light on how to define barycenters for probability distributions on general metric spaces. More formally, a *metric measure space* (*mm-space*) is a triple $\mathcal{X} = (X, d_X, \mu)$, where (X, d_X) is a Polish (complete and separable) metric space and μ is a Borel probability measure on (X, d_X) . The measure μ has *finite p -moments*, $p \geq 1$, if $\int_X d^p(x_0, y) d\mu(y) < \infty$ for some (and therefore all) $x_0 \in X$. The collection of all Borel probability measures on (X, d_X) with finite p -moments is denoted $\mathcal{B}(X, d_X; p)$. For $\mu \in \mathcal{B}(X, d_X; p)$, the *Fréchet variance function* of order p of \mathcal{X} , denoted $V_p: X \rightarrow \mathbb{R}$, is defined by

$$V_p(x) := \mathbb{E}_\mu[d_X^p(x, \cdot)] = \int_X d_X^p(x, y) d\mu(y). \quad (2)$$

The set of global minima of V_p (the global minimum may not be unique—see Example 1.1) is known as the *p -barycenter* of \mathcal{X} , also as the *Fréchet mean* for $p = 2$ and the *Fréchet median* for $p = 1$. As in [23], we replace V_p with its p th root $\sigma_p: X \rightarrow \mathbb{R}$, $\sigma_p(x) := (V_p(x))^{1/p}$, and call it the *p -deviation function* of \mathcal{X} . Clearly, the minimum sets of V_p and σ_p are the same, so we view p -barycenters as minimizers of σ_p . This is done because σ_p has better analytical properties than V_p . As local minimum sets are also important in our formulation, henceforth we relax the terminology to also include the local minima of V_p in the p -barycenter of \mathcal{X} .

Barycenters have received significant attention in the literature. The existence and uniqueness of global minima of V_2 on Hadamard manifolds (that is, complete, non-positively curved, simply-connected Riemannian manifolds) was already known to Cartan, whereas local minima of V_2 were first investigated in the Riemannian setting by Grove and Karcher [20], with subsequent developments in [21, 22, 26]. Barycenters for probability distributions on Wasserstein space have been investigated in [2, 28]. Other studies of barycenters include [7, 8, 1, 29, 4, 25], and [23] provides a persistent homology take on p -deviation functions. For additional historical remarks on developments related to barycenters, including applications, the reader may consult [1, 25].

In spite of the above, as is illustrated in Examples 1.1 and 1.2, the global minima of σ_p (or equivalently, V_p) can exhibit unstable behavior that makes them unsuited for data representation and analysis. Although not as pronounced, this instability persists even if we view the barycenter as comprising all local minima of σ_p . For this reason, this paper seeks to construct a representation of barycenters that is as simple as possible and yet robust, with guarantees of stability and consistency. This leads us to refine barycenters and define richer *barycentric merge tree (BMT)* representations of \mathcal{X} , show that they are stable, prove a consistency result for BMTs, and map a pathway to discrete models and computation. Roughly, the structure of the BMT representation of \mathcal{X} is as follows: the BMT is a rooted tree whose leaves represent the connected components of the local minimum sets of σ_p (i.e., of the p -barycenter), such that the tree structure captures interrelationships and connectivity properties of the sets of global and local minima. A BMT thus provides a more complete statistical summary of the *mm-space* (X, d_X, μ) than just the barycenter—see Figure 1 for an example on the circle.

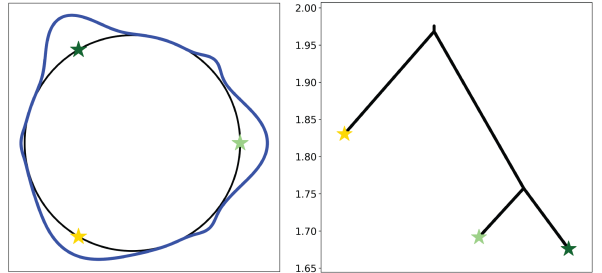


Figure 1: Barycentric merge tree example. **Left:** A probability density on the circle. The points marked by \star are local minima of σ_2 , with the darkest indicating the (global) Fréchet mean. **Right:** The barycentric merge tree summarizes the local minima, together with the shape of deviation function.

Example 1.1 (Instability of Means). This example illustrates the instability of global minima of σ_2 . Take the underlying metric space to be the unit circle endowed with geodesic distance and let μ

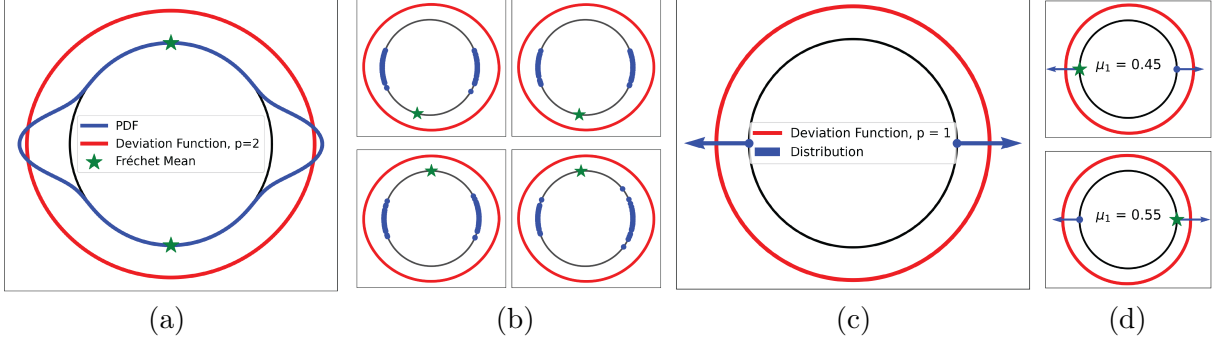


Figure 2: Instability of global minima of σ_p on the circle. **(a)** A pdf on the circle, its corresponding deviation function σ_2 , and the global minimizers of σ_2 . The deviation function and the pdf are both rescaled in this plot for visual clarity. **(b)** Four draws of 100 samples from the distribution shown in (a); σ_2 is plotted for each empirical distribution, along with its global minimizer, which varies wildly between samples. **(c)** A distribution on the circle consisting of equally weighted Dirac masses supported on antipodal points (represented by equal length arrows) and its deviation function σ_1 . Here, σ_1 is constant, so every point on the circle is a minimizer (i.e., a median). **(d)** Measures consisting of Dirac masses where the weight on the mass at $(1, 0)$ is given by μ_1 , together with their associated deviation functions σ_1 . If $\mu_1 > 1/2$, the unique median lies at $(1, 0)$, while the median lies at $(-1, 0)$ if $\mu_1 < 1/2$, indicated with a star in either case.

be the distribution with two modes shown in Figure 2(a), which also displays the deviation function σ_2 of μ and the Fréchet mean set formed by the north and south pole of the circle. We sample 100 points from μ and calculate the global Fréchet means of the associated empirical distributions. Figure 2(b) shows that the resulting Fréchet mean bounces between a point near the north pole and a point near the south pole, depending on the particular sample. This shows, qualitatively, that the Fréchet mean is unstable. Moreover, this same behavior persists as the number of samples is increased, as illustrated quantitatively in Example 4.6. \diamond

Example 1.2 (Instability of Medians). To see that medians are unstable, we once again consider an example where the metric space is the unit circle, endowed with geodesic distance. Let μ be a measure consisting of a weighted sum of Dirac masses—one with weight μ_1 at the point $(1, 0)$ and another with weight $\mu_2 = 1 - \mu_1$ at $(-1, 0)$. Parameterizing the circle by angle $\varphi \in [0, 2\pi)$, with $\varphi = 0$ corresponding to $(1, 0)$, it is not hard to show that σ_1 is given explicitly by

$$\sigma_1(\varphi) = \begin{cases} (\mu_1 - \mu_2)\varphi + \mu_2\pi & 0 \leq \varphi \leq \pi \\ (\mu_2 - \mu_1)\varphi + (2\mu_1 - \mu_2)\pi & \pi \leq \varphi < 2\pi. \end{cases} \quad (3)$$

If $\mu_1 = \mu_2 = 1/2$ then σ_1 is constant, as is illustrated in Figure 2(c), so all points on the circle are medians of μ . On the other hand, if $\mu_1 > 1/2$ then the unique minimizer of σ_1 (i.e., the median) lies at $(1, 0)$ and if $\mu_1 < 1/2$ then the unique minimizer lies at $(-1, 0)$. Examples are shown in Figure 2(d). \diamond

Example 1.3 (Stability of Barycentric Merge Trees). We reconsider the distributions from Example 1.1 and Figures 2(a)(b). Figure 3 shows the barycentric merge trees associated to the distributions. One can intuitively see that the resulting structures share a common structure; this stability property is a reflection of the Lipschitz bound established in Theorem 4.5. \diamond

1.2 Modes

The representation and estimation of the *modes* of a probability distribution on a metric space (X, d_X) are problems conceptually analogous to their counterparts for barycenters, as modes can

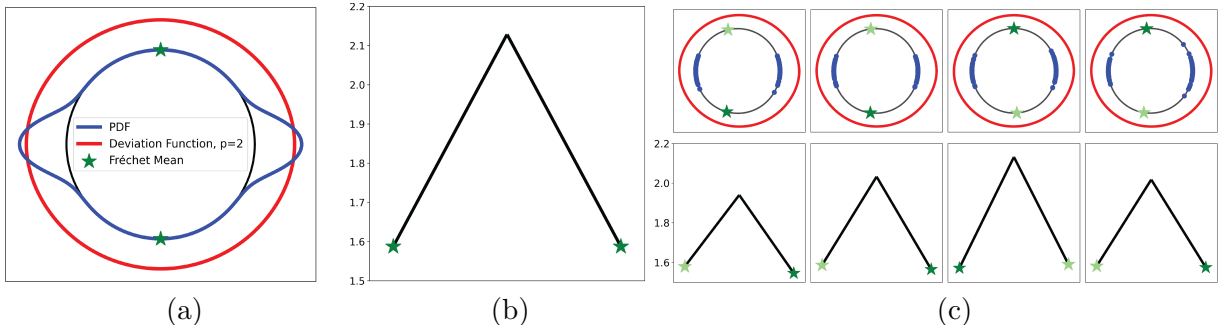


Figure 3: Stability of Barycentric Merge Trees on the circle. **(a)** A circle with a bimodal distribution, its deviation function σ_2 and the Fréchet mean set, as in Figure 2. **(b)** The BMT for the distribution in (a); the leaves of the tree correspond to the global minima of σ_2 (indicated by the stars), and the height of the merge point at the top corresponds to the maximum value of σ_2 . **(c)** BMTs for empirical distributions drawn from the pdf. Leaves of the trees correspond to marked points on the circles. Observe that the merge trees all have similar structure, reflecting the stability of the BMTs as summaries of the behavior of the deviation function.

be thought of as the most central points within pockets of probability mass. The shared centrality theme suggests a close connection between barycenters and modes, the main contrast being that, for modes, centrality takes a more localized form. However, even in very simple cases as Example 1.1, barycenters as defined above can lie in “data deserts”, away from regions of concentration of mass and contrary to the very concept of modes. For this reason, we broaden the definition of Fréchet variance and deviation functions to be able to frame the barycenter and mode problems as one. Instead of defining variance and deviation functions only with respect to the base metric d_X , in (2), we allow other (pseudo) metrics $\theta: X \times X \rightarrow \mathbb{R}$. Then, V_p takes the form

$$V_p(x) = \mathbb{E}_\mu[\theta^p(x, \cdot)] = \int_X \theta^p(x, y) d\mu(y). \quad (4)$$

As the notions of pockets of mass or clusters are inherently scale dependent, in mode detection, we employ diffusion distances θ derived from kernel functions $k: X \times X \rightarrow \mathbb{R}^+$ [12], as detailed in Section 5. The value $k(x, y)$ can be thought of as quantifying the level of communication between the points x and y , so that if both points lie in the support of the measure, mass near x and mass near y get clustered together by the kernel if $k(x, y)$ is sufficiently large. This produces a chaining effect that places a sequence of sufficiently θ -close local pockets of mass all into the same cluster. This diffusion distance formulation allows us to approach modes as a barycenter problem. For Riemannian manifolds

with the geodesic distance, the heat kernel associated with the Laplace-Beltrami operator gives a natural one-parameter family of kernels k_t , $t > 0$, to employ in mode analysis. We thus obtain a family of BMTs representing (X, d_X, μ) , parameterized by $t > 0$. In the tradition of scale space approaches to data analysis (cf. [30, 11]), different structural properties are captured across the range of scales and the family can also reveal scales at which the barycentric merge trees undergo “phase transitions”. Figure 4 illustrates the connection between diffusion distances and modes of

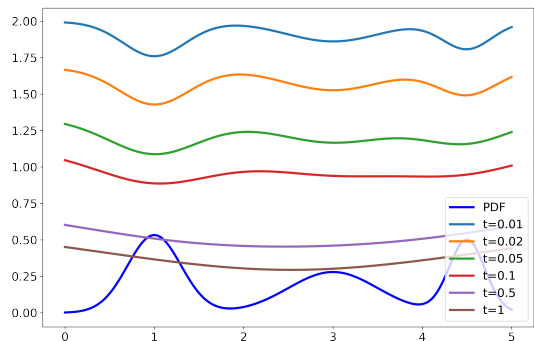


Figure 4: Fréchet variance functions associated with the heat kernel at different scales for a pdf on the real line.

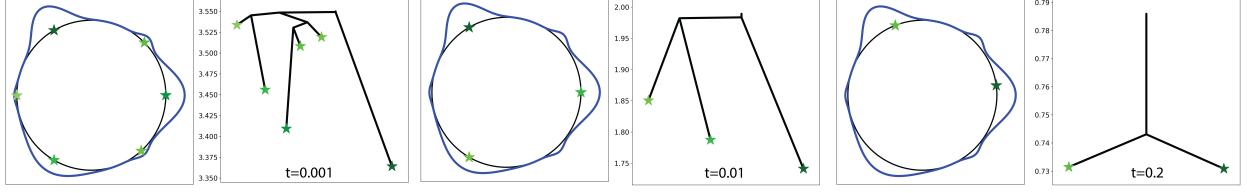


Figure 5: Merge trees for modes: each pair shows the distribution on the circle from Figure 1 with modes indicated by \star . The BMTs are calculated with respect to diffusion distances depending on an exponential kernel that has a scale parameter $t > 0$. The results shown are for various values of this parameter.

a distribution on the real line. The variance function V_2 is calculated with respect to diffusion distances derived from the heat kernel for several values of $t > 0$ (see Section 5 for details and also [15] for additional examples). Observe that, for small values of t , the local minima of the Fréchet variance now correspond to local maxima (i.e., local modes) of the pdf. This illustrates how the framework proposed in this paper simultaneously applies to the barycenter and mode estimation problems.

Example 1.4 (Modes and BMTs). Figure 5 shows the local mode detection pipeline applied to the circle distribution from Figure 1. Here an exponential kernel, depending on a scale parameter $t > 0$, is applied to the geodesic distance, which in turn determines the diffusion distance. Merge trees for the associated deviation function σ_2 are shown, together with the associated local modes on the circle (i.e., points corresponding to leaves on the trees). Increasing the scale parameter gives a coarser picture of the mode structure. \diamond

1.3 Barycentric Merge Trees

Continuous functions $f: X \rightarrow \mathbb{R}$ defined on connected domains can be succinctly represented by *merge trees* T_f , certain silhouettes of f visualized as rooted trees, that have been studied primarily from a metric perspective (cf. [33, 5, 13]). The present approach to barycentric merge trees differs from the purely metric view as it is based on a metric-measure formulation. To our knowledge, such a formulation has only been considered in a heuristic manner in the merge-tree literature, as in [13]. T_f is the quotient space of X under the equivalence relation $x \sim y$ if there exists $t \in \mathbb{R}$ such that $f(x) = f(y) = t$ and both x and y lie in the same connected component of the sublevel set $f^{-1}((-\infty, t])$. By construction, f descends to a function $\hat{f}: T_f \rightarrow \mathbb{R}$. Using merge heights for pairs of points in T_f , as measured by \hat{f} -values, one can equip T_f with a (pseudo) metric d_f [13, Definition 16] analogous to cophenetic distances for phylogenetic trees and dendograms [34]. This turns a merge tree into a functional (pseudo) metric space (T_f, d_f, \hat{f}) and a functional variant of the Gromov-Hausdorff distance provides a means for quantifying similarities and contrasts between two merge trees (T_f, d_f, \hat{f}) and (T_g, d_g, \hat{g}) , as done in [14] in the more general setting of Reeb graphs. A key difference between this type of metric and, say, the sup metric applied directly to f and g , is the geometry captured in a more explicit and compact form. The approach to merge trees in [33, 5] is different and based on interleaving distances.

The merge tree T_p associated with a p -deviation function $\sigma_p: X \rightarrow \mathbb{R}$ not only is equipped with a metric structure d_p and a function $\hat{\sigma}_p: T_p \rightarrow \mathbb{R}$, as described above, but also with a probability measure μ_p , namely, the pushforward of the original distributions μ on X to the quotient space T_p . We thus have a representation of the original mm -space $\mathcal{X} = (X, d_X, \mu)$ by a summary (functional) mm -space $(T_p, d_p, \mu_p, \hat{\sigma}_p)$. This additional probabilistic structure enables us to analyze variation

in barycentric merge trees in a *(functional) Gromov-Wasserstein framework* [32, 36, 3], instead of taking a purely metric approach. Our main stability result, obtained in Theorem 4.5, asserts that if μ and μ' are probability measures on X , then the distance between their barycentric merge trees, viewed as functional mm -spaces, admits an upper bound of the order of the Wasserstein distance between μ and μ' . Corollary 4.7 records the fact that this form of stability implies consistency, and we also obtain estimates for the rate of convergence of empirical barycentric merge trees to their theoretical population model. These rates are derived directly from the Stability Theorem and results by Weed and Bach on rates for Wasserstein convergence of empirical measures [38]. Stability and consistency for modes are included in these results because we frame modes as special cases of barycenters.

As the deviation functions for empirical measures are defined on the entire space X , we also propose a discretization scheme for empirical barycentric merge trees, which are the BMTs of practical interest. For X compact, starting from a finite δ -fine grid $V \subseteq X$, $\delta > 0$, we construct a combinatorial barycentric merge tree whose vertex set support a (functional) metric measure structure that is δ -close to the BMT of μ_n with respect to a Gromov-Wasserstein type distance. Since the combinatorial trees so obtained can be rather complex, with as many vertices as the cardinality of V , we also discuss a simplification method that gives a provably accurate approximation.

1.4 Organization

Section 2 defines Fréchet variance functions and p -deviation functions in a form that allows for a joint treatment of barycenters and modes, and also discusses connectivity properties on X that are needed to obtain stable barycentric merge trees. Section 3 constructs barycentric merge trees as (pseudo) metric measure spaces and examines some properties they satisfy. Section 4 proves the main results of the paper, namely, stability and consistency of barycentric merge trees. The application to analysis of modes is developed in Section 5, and Section 6 is devoted to discrete models. Section 7 closes the paper with a summary and some discussion.

Acknowledgements

The authors thank Nelson A. Silva for carefully reading the manuscript and suggesting several improvements to the text. This research was partially done while WM was visiting the Institute for Mathematical Sciences, National University of Singapore in 2024. TN was partially supported by NSF grants DMS-2107808 and DMS-2324962.

2 Preliminaries

In this paper, unless otherwise stated, (X, d_X) is a connected and locally path-connected Polish metric space (Polish meaning complete and separable). For spaces satisfying these connectivity hypotheses, we repeatedly use the fact that any open, connected subset $U \subseteq X$ is path connected. To simplify notation, for $w, z \in \mathbb{R}$, we adopt the abbreviations $w \vee z = \max\{w, z\}$ and $w \wedge z = \min\{w, z\}$ throughout the text.

2.1 Fréchet Variance and Deviation Functions

As explained in the Introduction, we take an approach to detection and estimation of modes of a probability distribution on a metric space (X, d_X) that requires versions of the Fréchet variance function based on distance functions other than d_X . For this reason, we define Fréchet variance

with respect to more general pseudo metrics $\theta: X \times X \rightarrow \mathbb{R}$, as this lets us frame modes as special cases of barycenters. A discussion of pseudo metrics derived from kernel functions and well suited to mode analysis is presented in Section 5.

Definition 2.1. Let $\mathcal{X} = (X, d_X, \mu)$ be an *mm-space* with $\mu \in \mathcal{B}(X, d_X; p)$, $p \geq 1$.

- (i) A pseudo-metric $\theta: X \times X \rightarrow \mathbb{R}$ is *L-admissible*, $L > 0$, if $\theta(x, y) \leq L d_X(x, y)$, $\forall x, y \in X$. We refer to such L as an *admissibility constant* for θ . We say that θ is *admissible* if it is L -admissible for some $L > 0$.
- (ii) The *Fréchet p-variance function* $V_p: X \rightarrow \mathbb{R}$ associated with an admissible θ is defined by

$$V_p(x) := \int_X \theta^p(x, y) d\mu(y).$$

The fact that μ has finite p -moments ensures that V_p is well defined. We omit θ from the Fréchet function notation to keep it simple, as the choice of θ should always be clear from the context.

- (iii) The *p-deviation function* $\sigma_p: X \rightarrow \mathbb{R}$ is defined as $\sigma_p(x) := (V_p(x))^{1/p}$.

The standard Fréchet variance function is that associated with $\theta = d_X$ and $p = 2$. The following proposition describes a basic property of deviation functions needed in our stability arguments.

Proposition 2.2. *If θ is an admissible pseudo metric and $\mu \in \mathcal{B}(X, d_X; p)$, then $|\sigma_p(x) - \sigma_p(y)| \leq \theta(x, y)$, for any $x, y \in X$.*

Proof. For $x, y \in X$, by the Minkowski inequality we have that

$$\begin{aligned} |\sigma_p(x) - \sigma_p(y)| &= \left| \left(\int_X \theta^p(x, z) d\mu(z) \right)^{1/p} - \left(\int_X \theta^p(y, z) d\mu(z) \right)^{1/p} \right| \\ &\leq \left(\int_X |\theta(x, z) - \theta(y, z)|^p d\mu(z) \right)^{1/p} \leq \left(\int_X \theta^p(x, y) d\mu(z) \right)^{1/p} = \theta(x, y). \end{aligned} \tag{5}$$

□

2.2 Connectivity Modulus

This section introduces the notions of *connectivity constant* and *connectivity modulus* for an admissible pseudo metric $\theta: X \times X \rightarrow \mathbb{R}$ on (X, d_X) . Let $I = [0, 1]$. Given $x, y \in X$, let $\Gamma(x, y)$ denote the collection of all (continuous) paths $\gamma: I \rightarrow (X, d_X)$ such that $\gamma(0) = x$ and $\gamma(1) = y$. Define the *merge distance function* $r_\theta: X \times X \rightarrow \mathbb{R}$ by

$$r_\theta(x, y) := \inf_{\gamma \in \Gamma(x, y)} \sup_{t \in I} \theta(x, \gamma(t)) \vee \theta(\gamma(t), y). \tag{6}$$

For $\theta = d_X$, we use the notation r_X for the merge distance function. Clearly,

$$\sup_{t \in I} \theta(x, \gamma(t)) \vee \theta(\gamma(t), y) \geq \theta(x, \gamma(0)) \vee \theta(\gamma(0), y) = \theta(x, y), \tag{7}$$

so that $r_\theta(x, y) \geq \theta(x, y)$, for any $x, y \in X$. In particular, $r_X \geq d_X$. By reversing path orientation, one readily verifies that r_θ is a symmetric function. Intuitively, $r_\theta(x, y)$ quantifies how far out, as measured by θ , we have to go from x and y to be able to connect x and y by a path.

Definition 2.3. Let (X, d_X) be a metric space, $\theta: X \times X \rightarrow \mathbb{R}$ an admissible pseudo metric, and $K > 0$.

- (i) K is a θ -connectivity constant for (X, d_X) if $r_\theta(x, y) \leq K d_X(x, y)$, $\forall x, y \in X$. If $\theta = d_X$, then $K \geq 1$ and we refer to K simply as a connectivity constant for (X, d_X) .
- (ii) The θ -connectivity modulus K_θ of (X, d_X) is defined as

$$K_\theta := \sup_{\substack{x, y \in X \\ x \neq y}} \frac{r_\theta(x, y)}{d_X(x, y)}.$$

For $\theta = d_X$, we write $K_\theta = K_X$ and call K_X the connectivity modulus of (X, d_X) .

If the θ -connectivity modulus is finite, K_θ is the smallest θ -connectivity constant for (X, d_X) .

Proposition 2.4. If (X, d_X) is a geodesic space, then $K_X = 1$.

Proof. We show that $r_X = d_X$, which implies that $K_X = 1$. As noted above, $r_X \geq d_X$. For the opposite inequality, let $\gamma_{x,y}: I \rightarrow X$ be a geodesic from x to y . Then,

$$d_X(x, \gamma_{x,y}(t)) \vee d_X(\gamma_{x,y}(t), y) \leq d_X(x, \gamma_{x,y}(t)) + d_X(\gamma_{x,y}(t), y) = d_X(x, y), \quad (8)$$

$\forall t \in I$. Taking the infimum over $\gamma \in \Gamma(x, y)$, we obtain $r_X(x, y) \leq d_X(x, y)$. \square

Proposition 2.5. Let $\theta: X \times X \rightarrow \mathbb{R}$ be an L -admissible pseudo metric. If $K \geq 1$ is a connectivity constant for (X, d_X) , then KL is a θ -connectivity constant for (X, d_X) ; that is, $r_\theta(x, y) \leq KL d_X(x, y)$.

Proof. By assumption, for any $x, y \in X$ and $\epsilon > 0$, there exists a path $\gamma \in \Gamma(x, y)$ such that $\sup_{t \in I} d_X(x, \gamma(t)) \vee d_X(\gamma(t), y) \leq \epsilon + K d_X(x, y)$. Then,

$$\sup_{t \in I} \theta(x, \gamma(t)) \vee \theta(\gamma(t), y) \leq L \sup_{t \in I} (d_X(x, \gamma(t)) \vee d_X(\gamma(t), y)) \leq L\epsilon + LK d_X(x, y). \quad (9)$$

Since $\epsilon > 0$ is arbitrary, we have $\sup_{t \in I} \theta(x, \gamma(t)) \vee \theta(\gamma(t), y) \leq KL d_X(x, y)$, which in turn implies that $r_\theta(x, y) \leq KL d_X(x, y)$. \square

3 Barycentric Merge Trees

This section introduces our main objects of study, barycentric merge trees. For $t \in \mathbb{R}$, we adopt the notation $A(t) := \sigma_p^{-1}((-\infty, t]) = \sigma_p^{-1}([0, t])$ for the sublevel sets of σ_p . The last equality holds because $\sigma_p \geq 0$.

Definition 3.1. The *barycentric merge tree (BMT)* of \mathcal{X} of order p for an admissible pseudo metric θ , $p \geq 1$, is denoted $T_p(\mathcal{X})$ and defined as the quotient space of X under the equivalence relation $x \sim y$ if there exists $t \in \mathbb{R}$ such that $\sigma_p(x) = \sigma_p(y) = t$ and x and y lie in the same connected component of $A(t)$. The quotient map is denoted $\alpha_p: X \rightarrow T_p(\mathcal{X})$.

Points in $T_p(\mathcal{X})$ are in one-to-one correspondence with the connected components of the sublevel sets of σ_p , as follows. For $x \in X$, let $t = \sigma_p(x)$ and $\alpha_p(x) = a \in T_p(\mathcal{X})$. Then, the point a represents the connected component C_a of $A(t)$ containing x . Clearly, C_a only depends on the equivalence class of x .

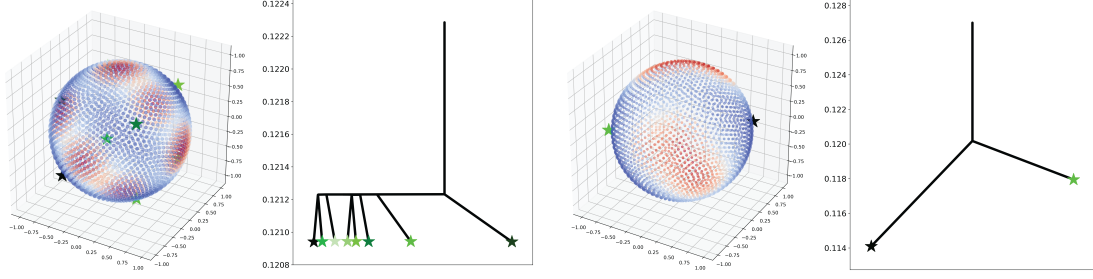


Figure 6: BMTs for distributions on the sphere (see Example 3.2). **Left:** Heat map representation of the pdf of a highly symmetric distribution on the 2-sphere, with modes at each intersection of the sphere with the coordinate axes. The BMT for $p = 2$ is shown, together with points corresponding to leaves on the sphere. **Right:** A less symmetric distribution on the 2-sphere with its BMT and points corresponding to the leaves.

Example 3.2 (BMTs on the Sphere). We illustrate the barycentric merge tree construction for distributions on the 2-sphere in Figure 6. In each case, we use the standard geodesic distance as the metric, and consider the associated deviation function σ_2 . The first example is for a highly symmetric distribution, given by a pdf which exponentially decays in distance from the set of points $\{(\pm 1, 0, 0), (0, \pm 1, 0), (0, 0, \pm 1)\}$. The resulting BMT has leaves corresponding to the faces of the standard cross-polytope, reflecting the symmetry of the measure. These points are the local minima of σ_2 . The leaves merge at a common height—corresponding to the unique local maximum value of the pdf—after which the sublevel sets of σ_2 are connected. The second example is a random transformation of the first, with no obvious symmetries, and results in a BMT with two leaves. Observe that in both examples, the computed local Fréchet means fall in low density areas, motivating the mode detection problem that we consider in Section 5.

All numerical examples in the paper are implemented via discrete approximations of the underlying spaces, following the method presented in Section 6. \diamond

By construction, the deviation function $\sigma_p: X \rightarrow \mathbb{R}$ descends to a function $\kappa_p: T_p(\mathcal{X}) \rightarrow \mathbb{R}$ such that the diagram

$$\begin{array}{ccc} X & \xrightarrow{\alpha_p} & T_p(\mathcal{X}) \\ & \searrow \sigma_p & \swarrow \kappa_p \\ & \mathbb{R} & \end{array} \quad (10)$$

commutes (this is the function which was denoted as $\hat{\sigma}_p$ in the introduction). $T_p(\mathcal{X})$ can be equipped with a poset (partially ordered set) structure that we now describe.

Definition 3.3. For $a \in T_p(\mathcal{X})$, let $C_a \subseteq X$ be the connected component of the sublevel set of σ_p represented by a .

- (i) The partial order \preceq is defined by $a \preceq b$ if $C_a \subseteq C_b$.
- (ii) A point $a \in T_p(\mathcal{X})$ is a *leaf* if it is a minimum point of the poset; that is, if $b \preceq a$, then $a = b$.
- (iii) Given $a, b, c \in T_p(\mathcal{X})$, c is a *merge point* for a and b if $a \preceq c$ and $b \preceq c$.

The partial ordering \preceq is compatible with the quotient topology on $T_p(\mathcal{X})$ in the sense that the graph of \preceq , given by

$$\{(a, b) \in T_p(\mathcal{X}) \times T_p(\mathcal{X}) : a \preceq b\}, \quad (11)$$

is a closed subspace of $T_p(\mathcal{X}) \times T_p(\mathcal{X})$. Thus, $T_p(\mathcal{X})$ is a *pospace* (partially ordered space), not just a poset.

Remark 3.4. The following properties satisfied by \preceq are readily verified:

- (i) The function $\kappa_p: T_p(\mathcal{X}) \rightarrow \mathbb{R}$ is monotonic; that is, $\kappa_p(a) \leq \kappa_p(b)$ if $a \preceq b$;
- (ii) For $a \in T_p(\mathcal{X})$, $C_a = \alpha_p^{-1}(\downarrow^a)$, where $\downarrow^a := \{b \in T_p(\mathcal{X}) : b \preceq a\}$ is the *principal lower set* of a ;
- (iii) If $a \preceq b$ and $a \preceq c$, then $b \preceq c$ or $c \preceq b$; that is, $T_p(\mathcal{X})$ has no branching points;
- (iv) If $a \preceq b$ and $\kappa_p(a) = \kappa_p(b)$, then $a = b$.

We now turn $T_p(\mathcal{X})$ into a (pseudo) *mm-space* starting with a (pseudo) metric on $T_p(\mathcal{X})$. For $a, b \in T_p(\mathcal{X})$, let

$$\Lambda(a, b) = \{c \in T_p(\mathcal{X}) : a \preceq c \text{ and } b \preceq c\} \quad (12)$$

be the *merge set* of a and b . Note that $\Lambda(a, b) \neq \emptyset$. Indeed, let $x_a, x_b \in X$ be such that $\alpha_p(x_a) = a$ and $\alpha_p(x_b) = b$, and let $\gamma: I \rightarrow X$ be a path from x_a to x_b . Such γ exists because X is path connected. Set $t_0 = \arg\max \sigma_p(\gamma(t))$, $x_0 = \gamma(t_0)$, and $c = \alpha_p(x_0)$. Then, $c \in \Lambda(a, b)$.

Definition 3.5 (cf. [13, 19]). The distance function $d_{p,\mathcal{X}}: T_p(\mathcal{X}) \times T_p(\mathcal{X}) \rightarrow \mathbb{R}$ is defined as

$$\begin{aligned} d_{p,\mathcal{X}}(a, b) &:= \inf_{c \in \Lambda(a, b)} (\kappa_p(c) - \kappa_p(a)) \vee (\kappa_p(c) - \kappa_p(b)) \\ &= \inf_{c \in \Lambda(a, b)} \kappa_p(c) - (\kappa_p(a) \wedge \kappa_p(b)). \end{aligned}$$

The next goal is to give an alternative description of $d_{p,\mathcal{X}}$ in terms of variation of σ_p along paths in X and show that $d_{p,\mathcal{X}}$ is indeed a pseudo metric. For $\gamma \in \Gamma(x, y)$, let

$$\begin{aligned} \rho(\gamma) &= \sup_{t \in I} (\sigma_p(\gamma(t)) - \sigma_p(x)) \vee (\sigma_p(\gamma(t)) - \sigma_p(y)) \\ &= \sup_{t \in I} \sigma_p(\gamma(t)) - (\sigma_p(x) \wedge \sigma_p(y)). \end{aligned} \quad (13)$$

Remark 3.6. $\rho(\gamma)$ only depends on the trace of γ , as it is invariant under reparameterizations of the curve in a very flexible sense. Namely, for any mapping $h: I \rightarrow I$ such that $h(0) = 0$ and $h(1) = 1$, the curve $\gamma' = \gamma \circ h$ satisfies $\rho(\gamma) = \rho(\gamma')$.

Definition 3.7. For $\mu \in \mathcal{B}(X, d_X; p)$, the *merge radius function* $m_{p,\mathcal{X}}: X \times X \rightarrow \mathbb{R}$ of $\mathcal{X} = (X, d_X, \mu)$ is defined as

$$m_{p,\mathcal{X}}(x, y) := \inf_{\gamma \in \Gamma(x, y)} \rho(\gamma) = \inf_{\gamma \in \Gamma(x, y)} \sup_{t \in I} \sigma_p(\gamma(t)) - (\sigma_p(x) \wedge \sigma_p(y)).$$

Proposition 3.8. Let $\mathcal{X} = (X, d_X, \mu)$ be an *mm-space* with $\mu \in \mathcal{B}(X, d_X; p)$, $p \geq 1$. Then, for any $x, x', y, y', z \in X$, the following statements hold:

- (i) $m_{p,\mathcal{X}}(x, z) \leq m_{p,\mathcal{X}}(x, y) + m_{p,\mathcal{X}}(y, z)$;
- (ii) if $\alpha_p(x) = \alpha_p(x')$, then $m_{p,\mathcal{X}}(x, x') = 0$;
- (iii) if $\alpha_p(x) = \alpha_p(x')$ and $\alpha_p(y) = \alpha_p(y')$, then $m_{p,\mathcal{X}}(x, y) = m_{p,\mathcal{X}}(x', y')$.

Proof. The argument is similar to that given in [14, Proposition 4] for a related result for Reeb spaces.

(i) Given $\gamma_1 \in \Gamma(x, y)$ and $\gamma_2 \in \Gamma(y, z)$, let $\gamma \in \Gamma(x, z)$ be the concatenation of γ_1 and γ_2 . Then,

$$\begin{aligned} \sup_{t \in I} \sigma_p(\gamma(t)) - \sigma_p(x) &= \left[\sup_{t \in I} \sigma_p(\gamma_1(t)) - \sigma_p(x) \right] \vee \left[\sup_{t \in I} \sigma_p(\gamma_2(t)) - \sigma_p(x) \right] \\ &= \left[\sup_{t \in I} \sigma_p(\gamma_1(t)) - \sigma_p(x) \right] \vee \left[\sup_{t \in I} \sigma_p(\gamma_2(t)) - \sigma_p(y) + \sigma_p(y) - \sigma_p(x) \right] \\ &\leq \left[\sup_{t \in I} \sigma_p(\gamma_1(t)) - \sigma_p(x) \right] + \left[\left(\sup_{t \in I} \sigma_p(\gamma_2(t)) - \sigma_p(y) \right) \right] \leq \rho(\gamma_1) + \rho(\gamma_2), \end{aligned} \quad (14)$$

for, $\sigma_p(y) - \sigma_p(x) \leq \sup_{t \in I} \sigma_p(\gamma_1(t)) - \sigma_p(x)$. Similarly, $\sup_{t \in I} \sigma_p(\gamma(t)) - \sigma_p(z) \leq \rho(\gamma_1) + \rho(\gamma_2)$. Therefore, $\rho(\gamma) \leq \rho(\gamma_1) + \rho(\gamma_2)$, which implies that

$$m_{p, \mathcal{X}}(x, z) = \inf_{\gamma \in \Gamma(x, z)} \rho(\gamma) \leq \inf_{\gamma_1 \in \Gamma(x, y)} \rho(\gamma_1) + \inf_{\gamma_2 \in \Gamma(y, z)} \rho(\gamma_2) = m_{p, \mathcal{X}}(x, y) + m_{p, \mathcal{X}}(y, z). \quad (15)$$

(ii) Let $t = \sigma_p(x) = \sigma_p(x')$ so that x and x' fall in the same connected component of the sublevel set $\sigma_p^{-1}((-\infty, t])$. For any $\epsilon > 0$, x and x' must fall in the same connected component C_ϵ of the open set $\sigma_p^{-1}((-\infty, t + \epsilon))$. Therefore, there is a path $\gamma \in \Gamma(x, y)$ whose image is contained in C_ϵ . This implies that $m_{p, \mathcal{X}}(x, x') \leq \rho(\gamma) < \epsilon$. Since $\epsilon > 0$ is arbitrary, $m_{p, \mathcal{X}}(x, x') = 0$.

(iii) By (i) and (ii),

$$m_{p, \mathcal{X}}(x, y) \leq m_{p, \mathcal{X}}(x, x') + m_{p, \mathcal{X}}(x', y') + m_{p, \mathcal{X}}(y', y) = m_{p, \mathcal{X}}(x', y'). \quad (16)$$

Similarly, $m_{p, \mathcal{X}}(x', y') \leq m_{p, \mathcal{X}}(x, y)$. This concludes the proof. \square

Proposition 3.8 implies that $m_{p, \mathcal{X}}$ induces a pseudo metric on $T_p(\mathcal{X})$; that is, the function $\hat{d}_{p, \mathcal{X}}: T_p(\mathcal{X}) \times T_p(\mathcal{X}) \rightarrow \mathbb{R}$ given by

$$\hat{d}_{p, \mathcal{X}}(\alpha_p(x), \alpha_p(y)) := m_{p, \mathcal{X}}(x, y) \quad (17)$$

is a well-defined pseudo metric.

Proposition 3.9. *If $\mu \in \mathcal{B}(X, d_X; p)$, $p \geq 1$, then $d_{p, \mathcal{X}} = \hat{d}_{p, \mathcal{X}}$. In particular, $d_{p, \mathcal{X}}$ is a pseudo metric.*

Proof. We first show that $d_{p, \mathcal{X}} \leq \hat{d}_{p, \mathcal{X}}$. Let $a, b \in T_p(\mathcal{X})$ and $x_a, x_b \in X$ be such that $\alpha_p(x_a) = a$ and $\alpha_p(x_b) = b$. Given $\epsilon > 0$, there is $\gamma \in \Gamma(x_a, x_b)$ such that $\sup_{t \in I} \sigma_p(\gamma(t)) - (\sigma_p(x) \wedge \sigma_p(y)) < \hat{d}_{p, \mathcal{X}}(a, b) + \epsilon$. Let $t_0 \in I$ be a point that realizes this supremum and set $c = \alpha_p(\gamma(t_0))$. Clearly, $\sigma_p(\gamma(t_0)) \geq \sigma_p(x) \vee \sigma_p(y)$ so that $c \in \Lambda(a, b)$ and

$$d_{p, \mathcal{X}}(a, b) \leq \kappa_p(c) - (\kappa_p(a) \wedge \kappa_p(b)) = \sigma_p(\gamma(t_0)) - (\sigma_p(x) \wedge \sigma_p(y)) < \hat{d}_{p, \mathcal{X}}(a, b) + \epsilon. \quad (18)$$

Since $\epsilon > 0$ is arbitrary, we obtain the desired inequality.

For the opposite inequality, given $\epsilon > 0$, let $c \in \Lambda(a, b)$ be such that $\kappa_p(c) - (\kappa_p(a) \wedge \kappa_p(b)) < d_{p, \mathcal{X}}(a, b) + \epsilon$. Let $x_a, x_b, x_c \in X$ be representatives of the equivalence classes $a, b, c \in T_p(\mathcal{X})$, respectively, and $t_c = \kappa_p(c)$. Then, x_a, x_b, x_c are contained in the same connected component C of the open set $\sigma_p^{-1}((-\infty, d_{p, \mathcal{X}}(a, b) + \epsilon))$. Since C is path connected, there is $\gamma \in \Gamma(x_a, x_b)$ whose image lies in C . This implies that $\hat{d}_{p, \mathcal{X}}(a, b) \leq \sup_{t \in I} \sigma_p(\gamma(t)) - \sigma_p(x_a) \wedge \sigma_p(x_b) < d_{p, \mathcal{X}}(a, b) + \epsilon$. Since $\epsilon > 0$ is arbitrary, we get $\hat{d}_{p, \mathcal{X}}(a, b) \leq d_{p, \mathcal{X}}(a, b)$. \square

One can show that if X is compact and $T_p(\mathcal{X})$ has finitely many leaves, then $d_{p,\mathcal{X}}$ metrizes the quotient topology on $T_p(\mathcal{X})$ (cf. [13]). This, however, may not be true in general. Nonetheless, we show that $d_{p,\mathcal{X}}$ has properties that make it well suited for our purposes: (a) the topology τ_p induced by $d_{p,\mathcal{X}}$ is fine enough for the mapping $\kappa_p: T_p(\mathcal{X}) \rightarrow \mathbb{R}$ to be continuous (1-Lipschitz, as a matter of fact); (b) τ_p is coarse enough for $\alpha_p: X \rightarrow T_p(\mathcal{X})$ to be continuous; and (c) $d_{p,\mathcal{X}}$ allows us to analyze BMT structural variation in a Gromov-Wasserstein type framework. As such, from this point on, we always assume that $T_p(\mathcal{X})$ is equipped with the metric $d_{p,\mathcal{X}}$.

Proposition 3.10. *If $\mu \in \mathcal{B}(X, d_X; p)$, then the following statements hold:*

- (i) *the map $\kappa_p: (T_p(\mathcal{X}), d_{p,\mathcal{X}}) \rightarrow \mathbb{R}$ is 1-Lipschitz;*
- (ii) *the map $\alpha_p: (X, d_X) \rightarrow (T_p(\mathcal{X}), d_{p,\mathcal{X}})$ is continuous.*

Proof. (i) Given $a, b \in T_p(\mathcal{X})$ and $\epsilon > 0$, Definition 3.5 ensures that there exists $c \in \Lambda(a, b)$ such that

$$(\kappa_p(c) - \kappa_p(a)) \vee (\kappa_p(c) - \kappa_p(b)) < d_{p,\mathcal{X}}(a, b) + \epsilon. \quad (19)$$

Since c is a merge point for a and b , we also have that $\kappa_p(a) \leq \kappa_p(c)$ and $\kappa_p(b) \leq \kappa_p(c)$. Therefore, $|\kappa_p(a) - \kappa_p(b)| < d_{p,\mathcal{X}}(a, b) + \epsilon$. Since $\epsilon > 0$ is arbitrary, $|\kappa_p(a) - \kappa_p(b)| \leq d_{p,\mathcal{X}}(a, b)$.

(ii) Let $U \subseteq T_p(\mathcal{X})$ be an open set and $\tilde{U} = \alpha_p^{-1}(U) \subseteq X$. To show that \tilde{U} is open, given $x \in \tilde{U}$ we construct an open neighborhood V of x such that $\alpha_p(V) \subseteq U$. Let $a = \alpha_p(x)$ and pick $\epsilon > 0$ such that $B(a, \epsilon) \subseteq U$, where $B(a, \epsilon)$ is the open ball of radius ϵ centered at a . Since X is locally path connected, there exists a path connected open neighborhood V of x with the property that $V \subseteq B(x, \epsilon/2L)$, where $L > 0$ is an admissibility constant for θ . We claim that $\alpha_p(V) \subseteq B(a, \epsilon) \subseteq U$. Indeed, given any $y \in V$, let $\beta \in \Gamma(x, y)$ be a path contained in V and thus in $B(x, \epsilon/2L)$. Proposition 2.2 ensures that σ_p is L -Lipschitz so that

$$\begin{aligned} |\sigma_p(\beta(s)) - \sigma_p(\beta(t))| &\leq |\sigma_p(\beta(s)) - \sigma_p(x)| + |\sigma_p(\beta(t)) - \sigma_p(x)| \\ &\leq Ld_X(\beta(s), x) + Ld_X(\beta(t), x) < \epsilon, \end{aligned} \quad (20)$$

for any $s, t \in I$. In particular, $\rho(\beta) = \sup_{t \in I} (\sigma_p(\beta(t)) - \sigma_p(x)) \vee (\sigma_p(\beta(t)) - \sigma_p(y)) < \epsilon$. This implies that

$$\hat{d}_{p,\mathcal{X}}(a, \alpha_p(y)) = \hat{d}_{p,\mathcal{X}}(\alpha_p(x), \alpha_p(y)) = \inf_{\gamma \in \Gamma} \rho(\gamma) \leq \rho(\beta) < \epsilon. \quad (21)$$

By Proposition 3.9, $d_{p,\mathcal{X}}(a, \alpha_p(y)) < \epsilon$, showing that $\alpha_p(y) \in B(a, \epsilon)$. This concludes the proof. \square

Definition 3.11. Let $\mu \in \mathcal{B}(X, d_X, p)$ and $\mathcal{X} = (X, d_X, \mu)$. The *metric-measure barycentric merge tree* of order p of \mathcal{X} is the triple $(T_p(\mathcal{X}), d_{p,\mathcal{X}}, \mu_p)$, where $\mu_p = \alpha_{p\#}(\mu)$ is the pushforward of μ under $\alpha_p: X \rightarrow T_p(\mathcal{X})$.

Henceforth, we always assume this *mm*-structure on $T_p(\mathcal{X})$ and simplify the terminology to *barycentric merge tree (BMT) of \mathcal{X}* if the choice of p (and the admissible pseudo metric θ) is clear from the context. We close this section with additional discussion of the metric properties of the map α_p under the assumption that (X, d_X) has finite connectivity modulus (see Definition 2.3).

Proposition 3.12. *If $K > 0$ is a connectivity constant for (X, d_X) and θ is L -admissible, then the quotient map $\alpha_p: (X, d_X) \rightarrow (T_p(\mathcal{X}), d_{p,\mathcal{X}})$ is KL -Lipschitz.*

Proof. Given $x, y \in X$ and $\epsilon > 0$, by Proposition 2.5 there is a path $\gamma_\epsilon \in \Gamma(x, y)$ such that

$$\sup_{t \in I} \theta(\gamma_\epsilon(t), x) \vee \theta(\gamma_\epsilon(t), y) < \epsilon + r_\theta(x, y) \leq \epsilon + KLd_X(x, y), \quad (22)$$

with $r_\theta(x, y)$ as in (6). Proposition 2.2 and (22) imply that $\rho(\gamma_\epsilon) < \epsilon + KLd_X(x, y)$. Therefore,

$$d_{p,\mathcal{X}}(\alpha_p(x), \alpha_p(y)) = \inf_{\gamma \in \Gamma(x, y)} \rho(\gamma) \leq \rho(\gamma_\epsilon) < \epsilon + KLd_X(x, y). \quad (23)$$

Since $\epsilon > 0$ is arbitrary, $d_{p,\mathcal{X}}(\alpha_p(x), \alpha_p(y)) \leq KLd_X(x, y)$, as claimed. \square

4 Stability and Consistency for Barycentric Merge Trees

The main goal of this section is to establish the stability of barycentric merge trees associated with probability measures $\mu \in \mathcal{B}(X, d_X; p)$, where the BMTs are constructed with respect to a fixed admissible pseudo metric θ . Since $T_p(\mathcal{X})$ is also equipped with a function $\kappa_p: T_p(\mathcal{X}) \rightarrow \mathbb{R}$ induced by the deviation function σ_p (see (10)), we address stability of the full functional barycentric merge tree $\mathcal{F}_p(\mathcal{X}) := (T_p(\mathcal{X}), d_{p,\mathcal{X}}, \mu_p, \kappa_p)$. In our stability and consistency results, variation in μ is quantified with the Wasserstein distance in (X, d_X) , from classical optimal transport theory [37], whereas variation in $\mathcal{F}_p(\mathcal{X})$ is measured with a functional version of Sturm's L_p -transportation distance, so we begin with a discussion of this distance.

4.1 Distances Between Functional Metric Measure Spaces

In [35], Sturm introduced L_p -transportation distances, $p \geq 1$, between mm -spaces building on Kantorovich's formulation of optimal transport distances that are frequently referred to in the literature as the *Wasserstein p -distances* w_p . Later Mémoli introduced a variant, termed *Gromov-Wasserstein p -distance*, based on expected distortions of probabilistic couplings [31]. As in some of the subsequent literature Sturm's version has also been called Gromov-Wasserstein, to avoid confusion, we refer to Sturm's formulation as the Kantorovich-Sturm p -distance $d_{KS,p}$ and denote Mémoli's version $d_{GW,p}$. The distance $d_{GW,p}$ has the virtue of being more amenable to computation and is a lower bound for $d_{KS,p}$; that is, $d_{GW,p}(\mathcal{Z}, \mathcal{Z}') \leq d_{KS,p}(\mathcal{Z}, \mathcal{Z}')$ [32, Theorem 5.1]. Because of this inequality, in studying the stability of barycentric merge trees, we use $d_{KS,p}$ -type metrics as they lead to stronger results that imply stability with respect to $d_{GW,p}$ -type distances.

The Kantorovich-Sturm distance can be extended to pseudo mm -spaces and described as follows. Let $\mathcal{Z} = (Z, d, \mu)$ and $\mathcal{Z}' = (Z', d', \mu')$ be (pseudo) mm -spaces, where μ and μ' have finite p -moments. Let $A \subseteq Z$ and $A' \subseteq Z'$ be the supports of μ and μ' , respectively. A *metric coupling* between \mathcal{Z} and \mathcal{Z}' is a (pseudo) metric $\delta: (Z \sqcup Z') \times (Z \sqcup Z') \rightarrow \mathbb{R}$ on the disjoint union $Z \sqcup Z'$ with the property that $\delta|_{A \times A} = d|_{A \times A}$ and $\delta|_{A' \times A'} = d'|_{A' \times A'}$. The set of all such metric couplings is denoted $M(\mathcal{Z}, \mathcal{Z}')$. A *probabilistic coupling* between μ and μ' is a Borel probability measure h on $Z \times Z'$ that marginalizes to μ and μ' ; that is, $\pi_\#(h) = \mu$ and $\pi'_\#(h) = \mu'$, where π and π' denote the projections to the first and second components, respectively. The set of all such probabilistic couplings is denoted $C(\mu, \mu')$.

Definition 4.1 ([35]). The (extended) *Kantorovich-Sturm p -distance*, $p \geq 1$, is defined as

$$d_{KS,p}(\mathcal{Z}, \mathcal{Z}') := \inf_{\substack{h \in C(\mu, \mu') \\ \delta \in M(\mathcal{Z}, \mathcal{Z}')}} \left(\int_{Z \times Z'} \delta^p(z, z') dh(z, z') \right)^{1/p}.$$

Since a merge tree $T_p(\mathcal{X})$ is also equipped with a function $\kappa_p: T_p(\mathcal{X}) \rightarrow \mathbb{R}$, we adopt a functional analogue of $d_{KS,p}$. For $f: Z \rightarrow \mathbb{R}$ and $f': Z' \rightarrow \mathbb{R}$, we define a Kantorovich-Sturm distance between the functional mm -spaces $\mathcal{F} = (Z, d, \mu, f)$ and $\mathcal{F}' = (Z', d', \mu', f')$.

Definition 4.2. The (extended) *functional Kantorovich-Sturm p -distance*, $p \geq 1$, is defined as

$$D_{KS,p}(\mathcal{F}, \mathcal{F}') := \inf_{\substack{h \in C(\mu, \mu') \\ \delta \in M(Z, Z')}} \left(\int_{Z \times Z'} \delta^p(z, z') dh(z, z') \right)^{1/p} \vee \left(\int_{Z \times Z'} |f(z) - f'(z')|^p dh(z, z') \right)^{1/p}.$$

We refer to the first term in the above maximum as the *structural offset* of the pair (δ, h) and to the second term as the *functional offset* of the coupling h . Clearly, by their definitions, $d_{KS,p}(Z, Z') \leq D_{KS,p}(\mathcal{F}, \mathcal{F}')$. The distance $D_{KS,p}$ is a variant of the *Fused Gromov-Wasserstein distance* of [36], which is a functional version of $d_{GW,p}$.

Metric couplings are closely tied to relations and correspondences between Z and Z' (a correspondence is a relation $R \subseteq Z \times Z'$ for which the projections $\pi: R \rightarrow Z$ and $\pi': R \rightarrow Z'$ are surjective). Here, we review a basic connection needed in the paper. Given a relation $\emptyset \neq R \subseteq Z \times Z'$, the *distortion* of R is defined as

$$dis(R) := \sup_{(x, x'), (y, y') \in R} |d(x, y) - d'(x', y')|. \quad (24)$$

For $r > 0$, define $\delta_r: (Z \sqcup Z') \times (Z \sqcup Z') \rightarrow \mathbb{R}$ by $\delta_r|_{Z \times Z} = d$, $\delta_r|_{Z' \times Z'} = d'$, and

$$\delta_r(z, z') = \delta_r(z', z) := r + \inf_{(w, w') \in R} d(z, w) + d'(w', z'), \quad (25)$$

for any $z \in Z$ and $z' \in Z'$.

Proposition 4.3 ([9], see also [3]). *If $\emptyset \neq R \subseteq Z \times Z'$ and $dis(R) \leq 2r$, then δ_r is a pseudo metric on $Z \sqcup Z'$.*

Clearly, $\delta_r(z, z') \geq r > 0$, for any $z \in Z$ and $z' \in Z'$. Thus, δ_r is a metric if and only if both d and d' are metrics.

4.2 Stability and Consistency

For $\mu, \mu' \in \mathcal{B}(X, d_X; p)$, we adopt the abbreviations $\mathcal{F}_p = (T_p, d_p, \mu_p, \kappa_p)$ and $\mathcal{F}'_p = (T'_p, d'_p, \mu'_p, \kappa'_p)$ for the functional barycentric merge trees of μ and μ' , respectively, constructed with respect to a fixed admissible $\theta: X \times X \rightarrow \mathbb{R}$. Similarly, we let $\mathcal{T}_p = (T_p, d_p, \mu_p)$ and $\mathcal{T}'_p = (T'_p, d'_p, \mu'_p)$ be the structural parts of \mathcal{F}_p and \mathcal{F}'_p , and σ_p and σ'_p the p -deviation functions of μ and μ' . To relate $D_{KS,p}(\mathcal{F}_p, \mathcal{F}'_p)$ with $w_p(\mu, \mu')$, we first construct a metric coupling between \mathcal{T}_p and \mathcal{T}'_p starting with the correspondence $R \subseteq T_p \times T'_p$ given by

$$R := \{(\alpha_p(x), \alpha'_p(x)): x \in X\}. \quad (26)$$

Given $r > 0$, let $\delta_r: (T_p \sqcup T'_p) \times (T_p \sqcup T'_p) \rightarrow \mathbb{R}$ be defined as described in (25): namely, (i) $\delta_r|_{T_p \times T_p} = d_p$; (ii) $\delta_r|_{T'_p \times T'_p} = d'_p$; and (iii) for $a \in T_p$ and $b \in T'_p$,

$$\delta_r(a, b) = \delta_r(b, a) := r + \inf_{x \in X} (d_p(a, \alpha_p(x)) + d'_p(\alpha'_p(x), b)). \quad (27)$$

Note that if $x_1, x_2 \in X$, then (27) implies that

$$\delta_r(\alpha_p(x_1), \alpha'_p(x_2)) \leq r + d_p(\alpha_p(x_1), \alpha_p(x_2)), \quad (28)$$

an inequality that is used below in the proof of the stability of BMTs.

Lemma 4.4 (The Coupling Lemma). *If the p -deviation functions satisfy $|\sigma_p(x) - \sigma'_p(x)| \leq r$, $\forall x \in X$, then δ_r defines a pseudo metric on $T_p \sqcup T'_p$. In particular, δ_r yields a metric coupling between \mathcal{T}_p and \mathcal{T}'_p .*

Proof. By Proposition 4.3, it suffices to check that $\text{dis}(R) \leq 2r$; that is, for any $x, y \in X$,

$$|d_p(\alpha_p(x), \alpha_p(y)) - d'_p(\alpha'_p(x), \alpha'_p(y))| \leq 2r. \quad (29)$$

We first show that for any curve $\gamma \in \Gamma(x, y)$, $|\rho(\gamma) - \rho'(\gamma)| \leq 2r$, where $\rho(\gamma)$ is as in (13) and $\rho'(\gamma)$ is its counterpart for σ'_p . Let $t_0 \in I$ be such that

$$\rho(\gamma) = (\sigma_p(\gamma(t_0)) - \sigma_p(x)) \vee (\sigma_p(\gamma(t_0)) - \sigma_p(y)). \quad (30)$$

Then, by the hypothesis on the deviation functions and the triangle inequality, we have that

$$\begin{aligned} \sigma_p(\gamma(t_0)) - \sigma_p(x) &= \sigma_p(\gamma(t_0)) - \sigma'_p(\gamma(t_0)) + \sigma'_p(\gamma(t_0)) - \sigma'_p(x) + \sigma'_p(x) - \sigma_p(x) \\ &\leq 2r + \sigma'_p(\gamma(t_0)) - \sigma'_p(x) \leq 2r + \sup_{t \in I} \sigma'_p(\gamma(t)) - \sigma'_p(x). \end{aligned} \quad (31)$$

Similarly,

$$\sigma_p(\gamma(t_0)) - \sigma_p(y) \leq 2r + \sup_{t \in I} \sigma'_p(\gamma(t)) - \sigma'_p(y). \quad (32)$$

Taking the maximum of (31) and (32), we obtain

$$\rho(\gamma) = (\sigma_p(\gamma(t_0)) - \sigma_p(x)) \vee (\sigma_p(\gamma(t_0)) - \sigma_p(y)) \leq 2r + \rho'(\gamma). \quad (33)$$

Symmetrically, we have that $\rho'(\gamma) \leq 2r + \rho(\gamma)$. Therefore, $|\rho(\gamma) - \rho'(\gamma)| \leq 2r$, as claimed. We now estimate the difference $d'_p(\alpha'_p(x), \alpha'_p(y)) - d_p(\alpha_p(x), \alpha_p(y))$. For a fixed curve $\gamma \in \Gamma(x, y)$, we have

$$\inf_{\gamma' \in \Gamma(x, y)} \rho'(\gamma') - \rho(\gamma) \leq \rho'(\gamma) - \rho(\gamma). \quad (34)$$

Therefore,

$$\begin{aligned} d'_p(\alpha'_p(x), \alpha'_p(y)) - d_p(\alpha_p(x), \alpha_p(y)) &= \inf_{\gamma' \in \Gamma(x, y)} \rho'(\gamma') - \inf_{\gamma \in \Gamma(x, y)} \rho(\gamma) \\ &= \sup_{\gamma \in \Gamma(x, y)} (\inf_{\gamma' \in \Gamma(x, y)} \rho'(\gamma') - \rho(\gamma)) \leq \sup_{\gamma \in \Gamma(x, y)} (\rho'(\gamma) - \rho(\gamma)) \leq 2r. \end{aligned} \quad (35)$$

Similarly, $d_p(\alpha_p(x), \alpha_p(y)) - d'_p(\alpha'_p(x), \alpha'_p(y)) \leq 2r$. This shows that (29) holds and concludes the proof. \square

Theorem 4.5 (Stability of BMTs). *Let (X, d_X) be a connected and locally path-connected Polish metric space and $\theta: X \times X \rightarrow \mathbb{R}$ an L -admissible pseudo metric, $L > 0$. If $\mu, \mu' \in \mathcal{B}(X, d_X; p)$ and $K \geq 1$ is a connectivity constant for (X, d_X) , then*

$$D_{KS,p}(\mathcal{F}_p, \mathcal{F}'_p) \leq L(1 + K)w_p(\mu, \mu').$$

In particular, $D_{KS,p}(\mathcal{F}_p, \mathcal{F}'_p) \leq 2w_p(\mu, \mu')$ if (X, d_X) is a geodesic space and $\theta = d_X$.

Proof. We begin the proof by showing that

$$|\sigma_p(x) - \sigma'_p(x)| \leq Lw_p(\mu, \mu'), \quad (36)$$

for all $x \in X$, using a standard argument that employs the Minkowski inequality and the marginal conditions of a measure coupling. Indeed, for any $h \in C(\mu, \mu')$, we have that

$$\begin{aligned}
|\sigma_p(x) - \sigma'_p(x)| &= \left| \left(\int_X \theta^p(x, y) d\mu(y) \right)^{1/p} - \left(\int_X \theta^p(x, y') d\mu'(y') \right)^{1/p} \right| \\
&= \left| \left(\int_{X \times X} \theta^p(x, y) dh(y, y') \right)^{1/p} - \left(\int_{X \times X} \theta^p(x, y') dh(y, y') \right)^{1/p} \right| \\
&\leq \left(\int_{X \times X} |\theta(x, y) - \theta(x, y')|^p dh(y, y') \right)^{1/p} \leq \left(\int_{X \times X} \theta^p(y, y') dh(y, y') \right)^{1/p} \\
&\leq L \left(\int_{X \times X} d_X^p(y, y') dh(y, y') \right)^{1/p},
\end{aligned} \tag{37}$$

Since the coupling h is arbitrary, we obtain

$$|\sigma_p(x) - \sigma'_p(x)| \leq L \inf_{h \in C(\mu, \mu')} \left(\int_{X \times X} d^p(y, y') dh(y, y') \right)^{1/p} = Lw_p(\mu, \mu'), \tag{38}$$

as claimed. Therefore, the Coupling Lemma applied with $r = Lw_p(\mu, \mu')$ ensures that δ_r , defined in (27), gives a coupling between d_p and d'_p . Also note that any $h \in C(\mu, \mu')$ induces a coupling $\bar{h} := (\alpha_p \times \alpha'_p)_\#(h) \in C(\mu_p, \mu'_p)$, where $\mu_p = \alpha_{p\#}(\mu)$ and $\mu'_p = \alpha'_{p\#}(\mu')$. Then, from inequality (28) and Proposition 3.12, we obtain

$$\delta_r(\alpha_p(x), \alpha'_p(y)) \leq r + d_p(\alpha_p(x), \alpha_p(y)) \leq Lw_p(\mu, \mu') + KLd_X(x, y). \tag{39}$$

Therefore, using the Minkowski inequality, we get the following estimate for the structural offset of the pair (δ_r, \bar{h}) :

$$\begin{aligned}
\left(\int_{T_p \times T'_p} \delta_r^p(\bar{x}, \bar{y}) d\bar{h}(\bar{x}, \bar{y}) \right)^{1/p} &= \left(\int_{X \times X} \delta_r^p(\alpha_p(x), \alpha'_p(y)) dh(x, y) \right)^{1/p} \\
&\leq Lw_p(\mu, \mu') + KL \left(\int_{X \times X} d_X^p(x, y) dh(x, y) \right)^{1/p}.
\end{aligned} \tag{40}$$

For the functional offset of \bar{h} , (38) and Proposition 2.2 yield

$$\begin{aligned}
\left(\int_{T_p \times T'_p} |\kappa_p(\bar{x}) - \kappa'_p(\bar{y})|^p d\bar{h}(\bar{x}, \bar{y}) \right)^{1/p} &= \left(\int_{X \times X} |\sigma_p(x) - \sigma'_p(y)|^p dh(x, y) \right)^{1/p} \\
&= \left(\int_{X \times X} |\sigma_p(x) - \sigma'_p(x) + \sigma'_p(x) - \sigma'_p(y)|^p dh(x, y) \right)^{1/p} \\
&\leq Lw_p(\mu, \mu') + L \left(\int_{X \times X} d_X^p(x, y) dh(x, y) \right)^{1/p},
\end{aligned} \tag{41}$$

an upper bound that is smaller than that for the structural offset in (40) because $K \geq 1$. Since the coupling h is arbitrary, it follows that

$$\begin{aligned}
D_{KS,p}(\mathcal{F}, \mathcal{F}') &\leq Lw_p(\mu, \mu') + KL \inf_{h \in C(\mu, \mu')} \left(\int_{X \times X} d_X^p(x, y) dh(x, y) \right)^{1/p} \\
&= L(1 + K)w_p(\mu, \mu'),
\end{aligned} \tag{42}$$

as claimed. For a geodesic space (X, d_X) and $\theta = d_X$, we can choose $L = 1$ and $K = 1$, as shown in Proposition 2.2. \square

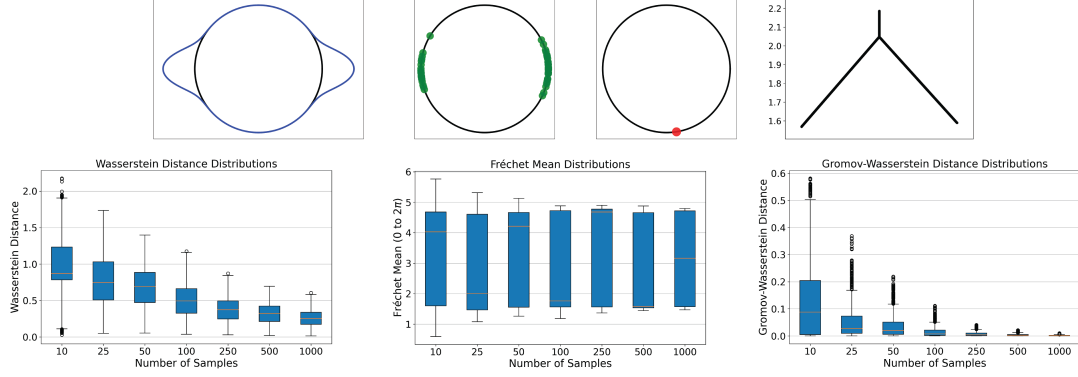


Figure 7: Quantitative stability of BMTs (see Example 4.6) **Top Row:** A summary of the experiment. We begin with a smooth bimodal distribution on the circle, which is then sampled n times ($n \in \{10, 25, 50, 100, 250, 500, 1000\}$), from which we compute a Fréchet mean (i.e., a point on the circle) and a barycentric merge tree ($p = 2$). This simulation is repeated 50 times for each n . **Bottom Row:** The distribution of Wasserstein distances between samples, treated as empirical distributions, for each value of n , shows convergence in number of samples. On the other hand, the Fréchet mean has a consistent spread for any number of samples. Finally, the distribution of Gromov-Wasserstein distances between BMTs for each n shows fast convergence.

Example 4.6 (Illustrating the Stability of BMTs). This example provides a quantitative illustration of the stability of BMTs and the lack thereof for (global) Fréchet means. We work with on the unit circle, endowed with geodesic distance, and with the bimodal distribution pictured in Figure 7. This distribution is sampled n times, for $n \in \{10, 25, 50, 100, 250, 500, 1000\}$, from which we define the associated empirical distribution. The global Fréchet mean (i.e., minimizer of σ_2) and the BMT, with respect to σ_2 , of this empirical distribution are then calculated, and this experiment is repeated 50 times for each value of n . Observe that, as n increases, the Wasserstein distance between the empirical distribution and the original measure converges to zero. Despite this fact, the variance in the resulting Fréchet means is essentially constant—the Fréchet mean bounces between roughly the north pole and south pole, indicating the instability of this statistic. On the other hand, the Gromov-Wasserstein distance between the associated BMTs converges to zero rather quickly as n increases—i.e., the BMTs are a stable invariant.

We note that the Gromov-Wasserstein distance (with $p = 2$) is used here, rather than the Kantorovich-Sturm distance, due to the availability of numerical solvers for the former; we use the Python Optimal Transport package for the calculation in this experiment [17]. Since the GW distance lower bounds the KS distance, the stability illustrated here is also guaranteed by the conclusion of Theorem 4.5. \diamond

For an mm -space $\mathcal{X} = (X, d_X, \mu)$, let $d_p^*(\mu)$ denote the upper p -Wasserstein dimension of \mathcal{X} (see [38]).

Corollary 4.7 (Empirical Estimation of FMTs). *Let $\mathcal{X} = (X, d_X, \mu)$ be an mm -space with $\mu \in \mathcal{B}(X, d_X; p)$, $p \geq 1$, where (X, d_X) is a connected and locally path connected Polish space, and $(x_i)_{i=1}^\infty$ be independent samples from μ . For $n > 0$, let $\mu_n = \sum_{i=1}^n \delta_{x_i}/n$ be the associated empirical measure and $\mathcal{X}_n = (X, d_X, \mu_n)$. If (X, d_X) has finite connectivity modulus and θ is L -admissible, then the following hold:*

- (i) (Consistency) $\lim_{n \rightarrow \infty} D_{KS,p}(\mathcal{F}_p(\mathcal{X}), \mathcal{F}(\mathcal{X}_n)) \rightarrow 0$, $(\otimes_\infty \mu)$ -almost surely;

(ii) (*Convergence Rate*) If $s > d_p^*(\mu)$, then there is a constant $C > 0$ such that

$$\mathbb{E}[D_{KS,p}(\mathcal{F}_p(\mathcal{X}), \mathcal{F}_p(\mathcal{X}_n))] \leq C \text{diam}(X) n^{-1/s},$$

where C depends only on s, p, L and the connectivity modulus of (X, d_X) .

Proof. (i) The statement follows from the Stability Theorem for barycentric merge trees and the facts that $\mu_n \rightarrow \mu$ weakly a. s. and w_p metrizes weak convergence of probability measures.

(ii) This follows from the Stability Theorem and the estimate $\mathbb{E}[w_p(\mu, \mu_n)] \leq C' n^{-1/s}$ by Weed and Bach under the hypothesis that $\text{diam}(X) \leq 1$, where C' depends only on s and p [38]. \square

5 Modes

We begin our discussion of robust detection and estimation of modes of a probability distribution on a metric space (X, d_X) with a review of diffusion distances on X (cf. [12]). This assumes a fixed reference measure ν on X ; for example, the volume measure on a Riemannian manifold.

Let $k: X \times X \rightarrow \mathbb{R}$ be a kernel function assumed to be continuous and non-negative. For each $x \in X$, define $k_x: X \rightarrow \mathbb{R}$ by $k_x(z) = k(x, z)$. Given $q \geq 1$, denote the q -norm on $L_q(X, \nu)$ by $\|\cdot\|_{\nu, q}$.

Definition 5.1. Let $k: X \times X \rightarrow \mathbb{R}$ be such that $k_x \in L_q(X, \nu)$, $\forall x \in X$. For $q \geq 1$, the *diffusion distance* $\theta_{k,q}: X \times X \rightarrow \mathbb{R}$ is defined as

$$\theta_{k,q}(x, y) := \|k_x - k_y\|_{\nu, q} = \left(\int_X |k(x, z) - k(y, z)|^q d\nu(z) \right)^{1/q}.$$

Clearly, $\theta_{k,q}$ defines a pseudo-metric on X because it is the pullback of the L_q -distance under the map $X \rightarrow L_q(X, \nu)$ given by $x \mapsto k_x$. Sometimes we drop explicit reference to q in the notation because it is fixed throughout.

Definition 5.2. Let $\mu \in \mathcal{B}(X, d_X, p)$, $p \geq 1$, and assume that $\theta_{k,q}$ is an admissible pseudo metric.

(i) A p -mode of $\mathcal{X} = (X, d_X, \mu)$ with respect to the kernel k is a connected component of a local minimum set of the p -deviation function $\sigma_{k,p}: X \rightarrow \mathbb{R}$ given by

$$\sigma_{k,p}(x) = \left(\int_X \theta_{k,q}^p(x, y) d\mu(y) \right)^{1/p}.$$

(ii) The p -mode merge tree of \mathcal{X} for the kernel k is the functional p -barycentric merge tree $\mathcal{F}_{k,p}(\mathcal{X})$ constructed with respect to the pseudo metric $\theta_{k,q}$.

Example 5.3 (Modes of Distributions on Shape Space). Consider the moduli space X of planar n -gons; each point in this space is an equivalence class of a closed n -sided polygon, considered up to rescaling, translation and rotation. We endow X with a Riemannian structure by utilizing a (perhaps surprising) correspondence between the moduli space and the Grassmann manifold $\text{Gr}_2(\mathbb{R}^n)$ of 2-planes in real n -space [24, 10]. The Grassmannian has a canonical Riemannian metric with an explicit formula for geodesic distance [16]. Denoting the induced distance on X by d_X , we then consider the kernel $k: X \times X \rightarrow \mathbb{R}$ defined by $k(x, y) = \exp(-10 \cdot d_X(x, y)^2)$. This kernel is used to compute mode merge trees for two distributions on the space of 10-gons, as follows.

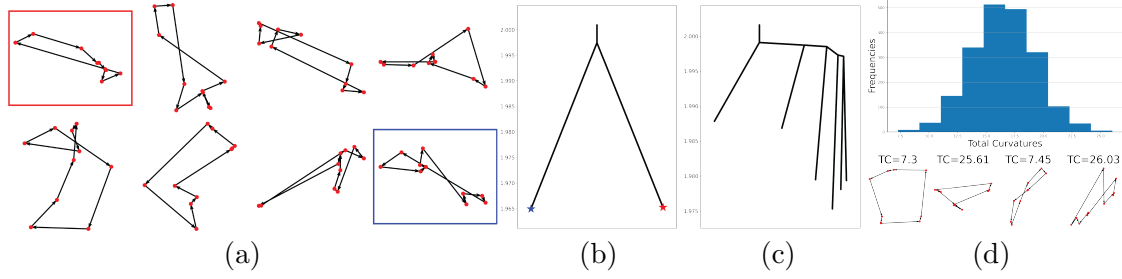


Figure 8: Mode trees in shape space (see Example 5.3 for details). **(a)** Random samples from the moduli space of 10-sided polygons. We work with a dataset of 2000 samples. **(b)** A pdf is defined as the sum of kernels which decay exponentially in the geodesic distance from the polygons indicated by boxes. The 2-mode tree is with respect to an exponential kernel; the leaves correspond to modes, which are located at the boxed polygons. **(c)** A new pdf is defined which gives higher weight to polygons with especially low or especially high total curvature. The lowest leaves of the mode tree correspond to the polygons shown in the bottom of **(d)**, whose total curvatures lie in the tails of the histogram in the top of **(d)**.

1. First, we fix two (equivalence classes of) polygons $x_0, x_1 \in X$ and define a pdf on X by starting with $y \mapsto \exp(-d(x_0, y)^2) + \exp(-d(x_1, y)^2)$, then renormalizing by total volume. Intuitively, the modes of the resulting distribution should be located at the points x_0 and x_1 ; this intuition is borne out computationally, as is shown in Figure 8.
2. Second, we define a pdf by renormalizing the function $x \mapsto (\text{TC}(x) - \widehat{\text{TC}})^4$, where $\text{TC}(x)$ is the *total curvature* of $x \in X$, or the sum of all of its turning angles, and $\widehat{\text{TC}}$ is the average value of total curvature. The resulting pdf assigns heavier weights to polygons with relatively low curvature or relatively high curvature. The mode tree shown in Figure 8 shows that the calculated local modes have extreme total curvature values.

As was indicated in Example 3.2, our numerics are performed by discretely approximating the underlying continuous spaces; in particular, we sample 2000 points from the Grassmannian by taking QR decompositions of random 10×2 matrices. We also remark that the displayed mode trees have been simplified by removing very short leaf edges, to improve visual clarity. \diamond

By definition, the leaves of $\mathcal{F}_{k,p}(\mathcal{X})$ represent the p -modes of \mathcal{X} with respect to the kernel k . Theorem 4.5 and Corollary 4.7 ensure that if (X, d_X) is a connected and locally path connected Polish space with finite connectivity modulus and $\theta_{k,q}$ is an admissible pseudo metric, then the p -mode merge trees for distributions with finite p -moments are stable and reliably can be estimated from sufficiently large independent samples. Corollary 4.7 also provides an estimate for the rate of convergence of mode merge trees associated with empirical measures. As such, we conclude this section by examining conditions on the kernel k that guarantee the admissibility of $\theta_{k,q}$.

Definition 5.4. The kernel $k: X \times X \rightarrow \mathbb{R}^+$ is *uniformly L -Lipschitz*, $L > 0$, if $|k(x, z) - k(y, z)| \leq Ld_X(x, y)$, for every $x, y, z \in X$.

Proposition 5.5. If the kernel $k: X \times X \rightarrow \mathbb{R}$ is uniformly L -Lipschitz and $\nu(X) < \infty$, then $\theta_{k,q}$ is $Lm_{q,\nu}$ -admissible for (X, d_X) , where $m_{q,\nu} = (\nu(X))^{1/q}$.

Proof. The assumption that k is uniform L -Lipschitz implies that

$$\theta_{k,q}(x, y) = \left(\int_X |k(x, z) - k(y, z)|^q d\nu(z) \right)^{1/q} \leq Ld_X(x, y) \left(\int_X d\nu(z) \right)^{1/q} = Lm_{q,\nu}d_X(x, y). \quad (43)$$

\square

Example 5.6. Let (M, d_M) be a closed (compact and without boundary) and connected Riemannian manifold equipped with the geodesic distance d_M . Denote by $k_t: M \times M \rightarrow \mathbb{R}$, $t > 0$, the heat kernel associated with the Laplace-Beltrami operator on M . By [27, Eq. (2.12)], there is a constant $C_t(M) > 0$ that varies continuously with $t > 0$ such that

$$|k_t(x, z) - k_t(y, z)| \leq C_t(M) d_M(x, y), \quad (44)$$

$\forall x, y, z \in M$. Thus, k_t is uniformly Lipschitz and Proposition 5.5 ensures that $\theta_{k,q}$ is admissible. Since (M, d_M) is a geodesic space, Theorem 4.5 guarantees that stability and consistency of mode merge trees hold for distributions on M . \diamond

Proposition 5.5 does not apply to the heat kernel on \mathbb{R}^d with ν the Lebesgue measure because of the finiteness condition on ν . Since this is an important case for applications, particularly for $q = 2$, in the next example we show by a direct calculation that, for $q = 2$, the diffusion distance on \mathbb{R}^d is admissible with respect to the Euclidean distance.

Example 5.7. Let $k_t: \mathbb{R}^d \times \mathbb{R}^d \rightarrow \mathbb{R}$, $t > 0$, be the heat kernel that is given by $k_t(x, y) = \frac{1}{(4\pi t)^{d/2}} \exp(-\|x - y\|^2/4t)$. For $q = 2$ and $t > 0$, denote the corresponding diffusion distance (with ν the Lebesgue measure) by $\theta_t: \mathbb{R}^d \times \mathbb{R}^d \rightarrow \mathbb{R}$. A routine calculation (see [15, Eq. 6]) shows that $\theta_t^2(x, y) = 2(\frac{1}{(8\pi t)^{d/2}} - k_{2t}(x, y))$. For a fixed pair (x, y) , parameterize the segment from x to y by $\beta(s) = (1 - s)x + sy$, $s \in I$, and let

$$g(s) := \theta_t^2(x, \beta(s)) = \frac{2}{(8\pi t)^{d/2}} \left(1 - \exp\left(-\frac{\|x - \beta(s)\|^2}{8t}\right) \right). \quad (45)$$

Then, $\theta_t^2(x, y) = g(1) - g(0) = \int_0^1 g'(s) ds$. The derivative of g is given by

$$g'(s) = \frac{(y - x) \cdot (\beta(s) - x)}{2t(8\pi t)^{d/2}} \exp\left(-\frac{\|x - \beta(s)\|^2}{8t}\right). \quad (46)$$

Since $\|\beta(s) - x\| \leq \|x - y\|$, from (46) we obtain

$$\theta_t^2(x, y) \leq \sup_{s \in I} |g'(s)| \leq \|x - y\|^2 / 2t(8\pi t)^{d/2}.$$

This implies that $\theta_t(x, y) \leq \|x - y\| / \sqrt{2t(8\pi t)^{d/4}}$, showing that θ_t is L_t -admissible with $L_t = 1/\sqrt{2t(8\pi t)^{d/4}}$. \diamond

Having shown in Example 5.7 that the diffusion distance θ_t is admissible, we now recall an interpretation given in [15, Eq. 10] of the Fréchet variance function $V_{p,t}: \mathbb{R}^d \rightarrow \mathbb{R}$, with respect to θ_t , for $p = 2$. At scale $t/2$, we have

$$V_{2,t/2}(x) = \int_{\mathbb{R}^d} d_{t/2}^2(x, y) d\mu(y) = \frac{2}{(4\pi t)^{d/2}} - 2u(t, x), \quad (47)$$

where $u(t, x)$ is the solution of the heat equation $\partial_t u = \Delta u$ with initial condition μ . In particular, up to a scaling factor 2, $V_{2,t/2}$ is an upside down version of the Gaussian kernel density estimator of μ at scale t . Therefore, in this special case, the modes of μ defined as the connected components of the local minimum sets of $V_{2,t/2}$ coincide with the view of modes as local maxima of kernel density estimators. Note, however, that in the proof that merge trees provide a stable and consistent representation of the modes of a distribution, we do not make assumptions such as local minima occurring at isolated points. Moreover, our approach also shows how to define modes for other values of p in a stable manner. For example, for $p = 1$, mode merge trees can be interpreted as local-global summaries of medians of probability measures.

6 Discrete Models

Corollary 4.7 establishes the consistency of BMT estimators derived from independent samples of a distribution on a connected and locally connected Polish space (X, d_X) . With an eye towards computation and applications, we now discuss provably accurate combinatorial approximations to barycentric merge trees associated with empirical measures on compact spaces. We begin with a discussion of general combinatorial BMTs and then apply the construction to empirical measures on (X, d_X) .

6.1 Combinatorial Barycentric Merge Trees

Let $G = (V, E)$ be a finite simple graph. We write (unoriented) edges as 2-element sets $\{v, w\} \in E$. In particular, loops $\{v, v\} = \{v\}$ are disallowed. We also assume that V is equipped with a metric d_V and a probability measure ω so that $\mathcal{V} = (V, d_V, \omega)$ is a finite *mm*-space. For $p \geq 1$, as before, define the p -deviation function $\sigma_p: V \rightarrow \mathbb{R}$ by

$$\sigma_p(v) = \left(\sum_{v' \in V} d_V^p(v, v') \omega(v') \right)^{1/p}. \quad (48)$$

For $t \in \mathbb{R}$, let $G_t \subseteq G$ be the subgraph spanned by the sublevel set $\sigma_p^{-1}([0, t]) \subseteq V$; that is, the largest subgraph of G whose vertex set is $\sigma_p^{-1}([0, t])$. On V , define an equivalence relation by $v \sim w$ if there exists $t \geq 0$ such that: (i) $\sigma_p(v) = \sigma_p(w) = t$ and (ii) v and w fall in the same connected component of G_t . The quotient $W_p = V / \sim$ is viewed as the vertex set of a (simple) graph $T_p = (W_p, E_p)$ whose edge set is defined by $\{[v], [w]\} \in E_p$ if $\{v, w\} \in E$ and $[v] \neq [w]$. Here, $[\cdot]$ denotes equivalence class. The quotient graph T_p is the *p-barycentric merge tree* of \mathcal{V} . Clearly, σ_p induces a function $\kappa_p: W_p \rightarrow \mathbb{R}$ such that $\sigma_p = \kappa_p \circ \alpha_p$, where $\alpha_p: V \rightarrow W_p$ is the quotient map.

As in the continuous case, we introduce a poset structure and a pseudo-metric on the node set of T_p . For $[v] \in W_p$, let $t = \kappa_p([v]) = \sigma_p(v)$ and $C_v \subseteq G$ be the connected component of G_t containing v . It is simple to verify that $C_{[v]}$ is independent of the choice of the representative v of the equivalence class. Define a partial order by $[v] \preceq [w]$ if $C_v \subseteq C_w$. A vertex $[z] \in W_p$ is a merge point for $[v]$ and $[w]$ if $[v] \preceq [z]$ and $[w] \preceq [z]$. The *merge set* $\Lambda[v, w]$ is defined as the collection of all merge points for $[v]$ and $[w]$. The function $d_p: W_p \times W_p \rightarrow \mathbb{R}$, given by

$$d_p([v], [w]) = \inf_{[z] \in \Lambda[v, w]} (\sigma_p(z) - \sigma_p(v)) \vee (\sigma_p(z) - \sigma_p(w)), \quad (49)$$

defines a pseudo-metric on W_p . As in Proposition 3.9, we can interpret $d_p([v], [w])$ in terms of (combinatorial) paths γ connecting v to w , where a path is given by a finite sequence $v = v_0, v_1, \dots, v_{m-1}, v_m = w$ of vertices of G such that $\{v_{i-1}, v_i\} \in E$, for every $1 \leq i \leq m$. The distance d_p may be expressed as $d_p([v], [w]) = \inf_{\gamma \in \Gamma_c(v, w)} \rho_c(\gamma)$, where $\Gamma_c(v, w)$ is the collection of all combinatorial paths from v to w and

$$\rho_c(\gamma) = \max_{v_i \in \gamma} (\sigma_p(v_i) - \sigma_p(v)) \vee (\sigma_p(v_i) - \sigma_p(w)). \quad (50)$$

Setting $\omega_p := \alpha_{p\#}(\omega)$, the pushforward of ω to W_p , we obtain a finite functional *mm*-space $(W_p, d_p, \omega_p, \kappa_p)$.

6.2 From Continuous to Discrete

Let (X, d_X) be a compact, connected and locally path connected metric space. We construct discrete graph models $G = (V, E)$ of X from finite δ -coverings $V \subseteq X$, $\delta > 0$. A subset $V =$

$\{v_1, \dots, v_m\} \subseteq X$ is a δ -covering if for each $x \in X$, there exists $v_i \in V$ such that $d_X(x, v_i) \leq \delta$. The parameter δ is to be viewed as controlling the desired accuracy of the approximation. We denote the induced metric on V by d_V . The edge set is defined by $\{v_i, v_j\} \in E$ if $d_V(v_i, v_j) \leq 3\delta$ and $i \neq j$.

Given a dataset $X_n = \{x_1, \dots, x_n\} \subseteq X$, let p_n be the normalized counting measure on X_n , given by $p_n(x_i) = 1/n$, and $\mu_n = \sum_{i=1}^n \delta_{x_i}/n$ be the associated empirical measure on X . Define a map $\phi: X_n \rightarrow V$, where $\phi(x_i)$ is arbitrarily chosen among the points $v_j \in V$ that satisfy $d_X(x_i, v_j) \leq \delta$. Define ω_n as the probability measure on V given by $\omega_n(v_i) = |\phi^{-1}(v_i)|/n$, the pushforward of p_n under ϕ . We refer to the finite mm -space $\mathcal{V}_n = (V, d_V, \omega_n)$ (with the underlying graph structure described above) as a *combinatorial δ -approximation* to $\mathcal{X}_n = (X, d_X, \mu_n)$. Further, if $\iota: V \hookrightarrow X$ denotes the inclusion map and $\nu_n = \iota_{\#}(\omega_n)$, we obtain yet another mm -space $\mathcal{W}_n = (X, d_X, \nu_n)$. We thus have three mm -spaces in play: (i) $\mathcal{X}_n = (X, d_X, \mu_n)$ which is the object of primary interest; (ii) $\mathcal{V}_n = (V, d_V, \omega_n)$ intended as a combinatorial proxy for \mathcal{X}_n ; and (iii) $\mathcal{W}_n = (X, d_X, \nu_n)$ that bridges the discrete and continuous models.

Note that, by construction, if $\sigma_{p, \mathcal{V}_n}: V \rightarrow \mathbb{R}$ and $\sigma_{p, \mathcal{W}_n}: X \rightarrow \mathbb{R}$ are the p -deviation functions of \mathcal{V}_n and \mathcal{W}_n , then $\sigma_{p, \mathcal{V}_n}(v) = \sigma_{p, \mathcal{W}_n}(v)$, for any $v \in V$. Moreover, $w_p(\mu_n, \nu_n) \leq \delta$, for any $p \geq 1$. Indeed, let $\psi: X_n \rightarrow X \times X$ be given by $\psi(x_i) = (x_i, \iota \circ \phi(x_i))$ and $h = \psi_{\#}(p_n)$. Then, $h \in C(\mu_n, \nu_n)$ and

$$w_p(\mu_n, \nu_n) \leq \left(\int_{X \times X} d_X^p(x, y) dh(x, y) \right)^{1/p} = \left(\frac{1}{n} \sum_{i=1}^n d_X^p(x_i, \phi(x_i)) \right)^{1/p} \leq \delta. \quad (51)$$

Therefore, under the assumptions of Theorem 4.5, the functional barycentric merge trees for \mathcal{X}_n and \mathcal{W}_n satisfy

$$D_{KS,p}(\mathcal{F}_p(\mathcal{X}_n), \mathcal{F}_p(\mathcal{W}_n)) \leq L(1 + K)\delta. \quad (52)$$

As such, to establish the validity of $\mathcal{F}_p(\mathcal{V}_n)$ as an approximation to $\mathcal{F}_p(\mathcal{X}_n)$, it suffices to obtain δ -controlled upper bounds for the Kantorovich-Sturm distance $D_{KS,p}(\mathcal{F}_p(\mathcal{V}_n), \mathcal{F}_p(\mathcal{W}_n))$.

Let $\alpha_{p, \mathcal{V}_n}: V \rightarrow T_p(\mathcal{V}_n)$ and $\alpha_{p, \mathcal{W}_n}: X \rightarrow T_p(\mathcal{W}_n)$ be the quotient maps and write the functional BMTs as $\mathcal{F}_p(\mathcal{V}_n) = (T_p(\mathcal{V}_n), d_{p, \mathcal{V}_n}, \omega_{p, n}, \kappa_{p, \mathcal{V}_n})$ and $\mathcal{F}_p(\mathcal{W}_n) = (T_p(\mathcal{W}_n), d_{p, \mathcal{W}_n}, \nu_{p, n}, \kappa_{p, \mathcal{W}_n})$, where $\omega_{p, n}$ and $\nu_{p, n}$ are the pushforwards of ω_n and ν_n under the quotient maps to the respective merge trees. As in the proof of the Stability Theorem, the key step in estimating $D_{KS,p}(\mathcal{F}_p(\mathcal{V}_n), \mathcal{F}_p(\mathcal{W}_n))$ is the construction of a metric coupling between d_{p, \mathcal{V}_n} and d_{p, \mathcal{W}_n} , starting from a relation $R \subseteq T_p(\mathcal{V}_n) \times T_p(\mathcal{W}_n)$, which we define as

$$R := \{(\alpha_{p, \mathcal{V}_n}(v), \alpha_{p, \mathcal{W}_n}(v)) : v \in V\}. \quad (53)$$

Lemma 6.1. *If $K \geq 1$ is a connectivity constant for (X, d_X) , θ is L -admissible, and $V \subseteq X$ a δ -covering of (X, d_X) , then the distortion of the relation R satisfies $\text{dis}(R) \leq KL\delta$.*

Proof. Let $v, w \in V$. Given a continuous path $\gamma \in \Gamma(v, w)$, take a grid $0 = t_0 < t_1 < \dots < t_N = 1$ fine enough so that $d_X(\gamma(t_i), \gamma(t_{i-1})) \leq \delta$, for every $1 \leq i \leq N$. Let $z_0 = v$, $z_N = w$, and for $0 < i < N$, set $z_i \in V$ be such that $d_X(\gamma(t_i), z_i) \leq \delta$. By the triangle inequality, $d_V(z_{i-1}, z_i) \leq 3\delta$, which implies that $\{z_{i-1}, z_i\}$ is an edge of $G = (V, E)$. Define β to be the combinatorial path $v = z_0, z_1, \dots, z_N = w$. Then, we have

$$\begin{aligned} \sigma_{p, \mathcal{V}_n}(z_i) - \sigma_{p, \mathcal{V}_n}(v) &= \sigma_{p, \mathcal{W}_n}(z_i) - \sigma_{p, \mathcal{W}_n}(\gamma(t_i)) + \sigma_{p, \mathcal{W}_n}(\gamma(t_i)) - \sigma_{p, \mathcal{W}_n}(v) \\ &\leq Ld_X(z_i, \gamma(t_i)) + \sup_{t \in I} \sigma_{p, \mathcal{W}_n}(\gamma(t)) - \sigma_{p, \mathcal{W}_n}(v) \\ &\leq L\delta + \sup_{t \in I} \sigma_{p, \mathcal{W}_n}(\gamma(t)) - \sigma_{p, \mathcal{W}_n}(v). \end{aligned} \quad (54)$$

Similarly,

$$\sigma_{p, \mathcal{V}_n}(z_i) - \sigma_{p, \mathcal{V}_n}(w) \leq L\delta + \sup_{t \in I} \sigma_{p, \mathcal{W}_n}(\gamma(t)) - \sigma_{p, \mathcal{W}_n}(w). \quad (55)$$

Therefore,

$$\begin{aligned}\rho_c(\beta) &= \max_i (\sigma_{p,\mathcal{V}_n}(z_i) - \sigma_{p,\mathcal{V}_n}(v) \vee \sigma_{p,\mathcal{V}_n}(z_i) - \sigma_{p,\mathcal{V}_n}(w)) \\ &\leq L\delta + \sup_{t \in I} (\sigma_{p,\mathcal{W}_n}(\gamma(t)) - \sigma_{p,\mathcal{W}_n}(v)) \vee (\sigma_{p,\mathcal{W}_n}(\gamma(t)) - \sigma_{p,\mathcal{W}_n}(w)) = L\delta + \rho(\gamma).\end{aligned}\quad (56)$$

Taking the infimum over γ , we obtain

$$d_{p,\mathcal{V}_n}(\alpha_{p,\mathcal{V}_n}(v), \alpha_{p,\mathcal{V}_n}(w)) \leq L\delta + d_{p,\mathcal{W}_n}(\alpha_{p,\mathcal{W}_n}(v), \alpha_{p,\mathcal{W}_n}(w)), \quad (57)$$

for any $v, w \in V$. Conversely, let an edge path $\beta \in \Gamma_c(v, w)$ be given by the sequence $v = z_0, z_1, \dots, z_N = w$ in V . Given $\epsilon > 0$, for each $1 \leq i \leq N$, let γ_i be a path from z_{i-1} to z_i with the property that

$$\sup_t (d_X(v, \gamma_i(t)) \vee d_X(\gamma_i(t), w)) \leq \epsilon + Kd_X(z_{i-1}, z_i), \quad (58)$$

whose existence is guaranteed by the fact that K is a connectivity constant for (X, d_X) . Concatenating all γ_i , $1 \leq i \leq N$, we obtain $\gamma \in \Gamma(v, w)$ such that for each $t \in I$, there is $i(t) \in \{0, 1, \dots, N\}$ such that $d_X(\gamma(t), z_{i(t)}) \leq \epsilon + K\delta$. Hence,

$$\begin{aligned}\sigma_{p,\mathcal{W}_n}(\gamma(t)) - \sigma_{p,\mathcal{W}_n}(v) &= \sigma_{p,\mathcal{W}_n}(\gamma(t)) - \sigma_{p,\mathcal{W}_n}(z_{i(t)}) + \sigma_{p,\mathcal{V}_n}(z_{i(t)}) - \sigma_{p,\mathcal{V}_n}(v) \\ &\leq Ld_X(\gamma(t), z_{i(t)}) + \max_i \sigma_{p,\mathcal{V}_n}(z_i) - \sigma_{p,\mathcal{V}_n}(v) \leq \epsilon + KL\delta + \rho_c(\beta).\end{aligned}\quad (59)$$

An identical argument shows that

$$\sigma_{p,\mathcal{W}_n}(\gamma(t)) - \sigma_{p,\mathcal{W}_n}(w) \leq \epsilon + KL\delta + \rho_c(\beta). \quad (60)$$

Since $\epsilon > 0$ is arbitrary, taking the infimum over β and using (59) and (60), we obtain

$$d_{p,\mathcal{W}_n}(\alpha_{p,\mathcal{W}_n}(v), \alpha_{p,\mathcal{W}_n}(w)) \leq KL\delta + d_{p,\mathcal{V}_n}(\alpha_{p,\mathcal{V}_n}(v), \alpha_{p,\mathcal{V}_n}(w)), \quad (61)$$

for any $v, w \in V$. Combining (57) and (61), since $K \geq 1$, we get $\text{dis}(R) \leq KL\delta$, as claimed. \square

Theorem 6.2. *If $K \geq 1$ is a connectivity constant for the compact metric space (X, d_X) , θ is L -admissible, and $V \subseteq X$ a δ -covering of (X, d_X) , then $D_{KS,p}(\mathcal{F}_p(\mathcal{V}_n), \mathcal{F}_p(\mathcal{W}_n)) \leq KL\delta/2$.*

Proof. Proposition 4.3 and Lemma 6.1 imply that, for $r = KL\delta/2$, there is a metric coupling $\delta_r \in M(d_{p,\mathcal{V}_n}, d_{p,\mathcal{W}_n})$ such that for $\bar{v} \in T_p(\mathcal{V}_n)$ and $\bar{x} \in T_p(\mathcal{W}_n)$,

$$\delta_r(\bar{v}, \bar{x}) = \delta_r(\bar{x}, \bar{v}) = r + \inf_{w \in V} d_{p,\mathcal{V}_n}(\bar{v}, \alpha_{p,\mathcal{V}_n}(w)) + d_{p,\mathcal{W}_n}(\alpha_{p,\mathcal{W}_n}(w), \bar{x}). \quad (62)$$

In particular, $\delta_r(\alpha_{p,\mathcal{V}_n}(v), \alpha_{p,\mathcal{W}_n}(v)) = r$.

Let $\Delta: V \rightarrow V \times X$ be given by $\Delta(v) = (v, v)$. Since $\nu_n = \imath_{\#}(\omega_n)$, $h = \Delta_{\#}(\omega_n)$ gives a coupling between ω_n and ν_n , which in turn, induces a coupling $\bar{h} := (\sigma_{p,\mathcal{V}_n} \times \sigma_{p,\mathcal{W}_n})_{\#}(h) \in C(\omega_{p,n}, \nu_{p,n})$. Since the coupling h is diagonal, by Proposition 3.12 and (6.2), the structural offset of (δ_r, \bar{h}) satisfies

$$\left(\int_{T_p(\mathcal{V}_n) \times T_p(\mathcal{W}_n)} \delta_r^p(\bar{v}, \bar{x}) d\bar{h}(\bar{v}, \bar{x}) \right)^{1/p} = \left(\int_V \delta_r^p(\alpha_{p,\mathcal{V}_n}(v), \alpha_{p,\mathcal{W}_n}(v)) d\omega_n(v) \right)^{1/p} \leq r. \quad (63)$$

As $\sigma_{p,\mathcal{V}_n}(v) = \sigma_{p,\mathcal{W}_n}(v)$, $\forall v \in V$, the functional offset of \bar{h} vanishes. Indeed,

$$\int_{T_p(\mathcal{V}_n) \times T_p(\mathcal{W}_n)} |\kappa_{p,\mathcal{V}_n}(\bar{v}) - \kappa_{p,\mathcal{W}_n}(\bar{x})|^p d\bar{h}(\bar{v}, \bar{x}) = \int_V |\sigma_{p,\mathcal{V}_n}(v) - \sigma_{p,\mathcal{W}_n}(v)|^p d\omega_n(v) = 0. \quad (64)$$

Therefore, $D_{KS,p}(\mathcal{F}_p(\mathcal{V}_n), \mathcal{F}_p(\mathcal{W}_n)) \leq r = KL\delta/2$. \square

Corollary 6.3. *If $K \geq 1$ is a connectivity constant for a compact metric space (X, d_X) , θ is L -admissible, and $V \subseteq X$ a δ -covering of (X, d_X) , then $D_{KS,p}(\mathcal{F}_p(\mathcal{V}_n), \mathcal{F}_p(\mathcal{X}_n)) \leq C_{K,L} \delta$, where $C_{K,L} = L + 3KL/2$.*

Proof. This follows from (52) and Theorem 6.2. \square

6.3 Binning

Section 6.2 constructs combinatorial approximations to barycentric merge trees with accuracy guarantees. A drawback of the construction is that, generically, the values of a p -deviation function on the nodes of the tree are all distinct, making the associated BMT rather large and complex with many small branches. Such merge trees do not achieve the goal of providing a concise summary of the original probability distribution. For this reason, we introduce an additional binning step to simplify the function $\sigma_{p,\mathcal{V}_n}: V \rightarrow \mathbb{R}$ before constructing the merge tree. Given $\varepsilon > 0$, define $\tau_\varepsilon: V \rightarrow \mathbb{R}$ by $\tau_\varepsilon(v) = \varepsilon \lfloor \sigma_{p,\mathcal{V}_n}(v)/\varepsilon \rfloor$, an approximation to σ_{p,\mathcal{V}_n} that satisfies $|\sigma_{p,\mathcal{V}_n}(v) - \tau_\varepsilon(v)| \leq \varepsilon$, for every $v \in V$. Here, $\lfloor \cdot \rfloor$ denotes the floor function. This has the effect of approximating σ_{p,\mathcal{V}_n} by a function that has constant value $i\varepsilon$ on sets of the form $\sigma_{p,\mathcal{V}_n}^{-1}([i\varepsilon, (i+1)\varepsilon)) \subseteq V$, where i is an arbitrary non-negative integer.

Construct a combinatorial functional merge tree $\mathcal{F}_{p,\varepsilon}(\mathcal{V}_n)$, viewed as an approximation to $\mathcal{F}_p(\mathcal{V}_n)$, from the same graph mm -structure (V, E, d_V, ω_n) only replacing σ_{p,\mathcal{V}_n} with τ_ε .

Theorem 6.4. *For any $\varepsilon > 0$, $D_{KS,p}(\mathcal{F}_p(\mathcal{V}_n), \mathcal{F}_{p,\varepsilon}(\mathcal{V}_n)) \leq \varepsilon$.*

Proof. We use the abbreviations $\mathcal{F}_p(\mathcal{V}) = (T, d, \omega_p, \kappa)$, $\mathcal{F}_{p,\varepsilon}(\mathcal{V}_n) = (T', d', \omega'_p, \kappa')$, $\sigma = \sigma_{p,\mathcal{V}_n}$, and also $\alpha: V \rightarrow T$ and $\alpha': V \rightarrow T'$ for the quotient maps. Since $|\sigma(v) - \tau_\varepsilon(v)| \leq \varepsilon$, for every $v \in V$, arguing as in Lemma 4.4, we have that δ_ε given on pairs $(a, b) \in T \times T'$ by

$$\delta_\varepsilon(a, b) = d_\varepsilon(b, a) := \varepsilon + \inf_{v' \in V} (d(a, \alpha(v')) + d'(\alpha'(v'), b)). \quad (65)$$

defines a coupling $\delta_\varepsilon \in M(d, d')$ for which $\delta_\varepsilon(\alpha(v), \alpha'(v)) = \varepsilon$, $\forall v \in V$. As in the proof of Theorem 6.2, let $h = \Delta_\#(\omega_n)$, where $\Delta: V \rightarrow V \times V$ is the diagonal map, and $\bar{h} \in C(\omega_p, \omega'_p)$ be given by $\bar{h} = (\alpha, \alpha')_\#(h)$. Then, the structural offset of $(\delta_\varepsilon, \bar{h})$ satisfies

$$\left(\int_{T \times T'} \delta_\varepsilon^p(\bar{v}, \bar{w}) d\bar{h}(\bar{v}, \bar{w}) \right)^{1/p} = \left(\int_V \delta_\varepsilon^p(\alpha(v), \alpha'(v)) d\omega_n(v) \right)^{1/p} = \varepsilon. \quad (66)$$

Similarly,

$$\left(\int_{T \times T'} |\kappa(\bar{v}) - \kappa'(\bar{w})|^p d\bar{h}(\bar{v}, \bar{w}) \right)^{1/p} = \left(\int_V |(\sigma(v) - \tau_\varepsilon(v))^p| d\omega_n(v) \right)^{1/p} \leq \varepsilon. \quad (67)$$

Therefore, $D_{KS,p}(\mathcal{F}_p(\mathcal{V}_n), \mathcal{F}_{p,\varepsilon}(\mathcal{V}_n)) \leq \varepsilon$. \square

7 Summary and Concluding Remarks

As the p -barycenters and modes of a probability distribution μ on a metric space (X, d_X) exhibit an unstable behavior, this paper introduced a functional merge tree representation of barycenters and modes that is provably stable and can be estimated reliably from data. This has been done at the generality of all Borel probability measures on a Polish metric space with finite p -moments. The leaves of a barycentric merge tree represent the connected components of the local minimum sets of

the p -deviation function (or equivalently, the Fréchet p -variance function) of (X, d_X, μ) . The merge tree provides a sketch of the interrelationships between the various sublevel sets of the p -deviation function, in particular, the merging patterns of the barycenters or modes of μ , thus providing a more complete summary of (X, d_X, μ) than the barycenters alone. A unifying framework was developed for the investigation of both the barycenter and mode problems, with modes viewed as special types of barycenters associated with diffusion distances. The main results are a stability theorem and a consistency result for barycentric merge trees, which were proven in a Gromov-Wasserstein type framework. The paper also presented a pathway to discretization and computation via combinatorial merge trees. The accuracy guarantees for these discrete approximations were established in Section 6.2 only for empirical measures as this sufficed for our purposes because Corollary 4.7 guarantees that the BMT for a more general probability measure μ can be approximated by those for empirical measures. Nonetheless, we note that the argument in Section 6.2 can be adapted to prove a similar approximation result more directly for a general distribution μ .

The choice of merge trees was largely guided by the goal of achieving stability keeping the representation of barycenters as simple as possible. Similar representations can likely be obtained through Reeb graphs (cf. [14]) at the expense of increasing the complexity of both the model and computations. The focus of the paper was on foundational aspects of stable representations of barycenters leaving questions specific to cases such as distributions on Riemannian manifolds, length spaces, networks, or Wasserstein spaces for further investigation.

While we provided several computational examples in this paper, their primary function was to provide intuition and enhance exposition. Developing a full-fledged, efficient numerical framework for extracting BMTs from real data remains an important direction of future research. The figures in the paper can be reproduced from the open access code available at our GitHub repository (<https://github.com/trneedham/Barycentric-Merge-Trees>).

References

- [1] B. Afsari. Riemannian L_p center of mass: existence, uniqueness, and convexity. *Proc. Amer. Math. Soc.*, 139:655–673, 2011.
- [2] M. Agueh and G. Carlier. Barycenters in the Wasserstein space. *SIAM J. Math. Anal.*, 43(2):904–924, 2011.
- [3] S. Anbouhi, W. Mio, and O. B. Okutan. On metrics for analysis of functional data on geometric domains. *Found. Data Sci.*, 7(3):671–704, 2025.
- [4] M. Arnaudon and L. Miclo. Means in complete manifolds: uniqueness and approximation. *ESAIM: Probability and Statistics*, 18:185–206, 2014.
- [5] K. Beketayev, D. Yeliussizov, D. Morozov, G. Weber, and B. Hamann. Measuring the distance between merge trees. In *Topological Methods in Data Analysis and Visualization III*, pages 151–166, 2014.
- [6] M. Berger. *A Panoramic View of Riemannian Geometry*. Springer-Verlag, 2003.
- [7] R. Bhattacharya and V. Patrangenaru. Large sample theory of intrinsic and extrinsic sample means on manifolds. I. *Ann. Statist.*, 31:1–29, 2003.
- [8] R. Bhattacharya and V. Patrangenaru. Large sample theory of intrinsic and extrinsic sample means on manifolds. II. *Ann. Statist.*, 33:1225–1259, 2005.

- [9] D. Burago, Y. Burago, and S. Ivanov. *A Course in Metric Geometry*. American Mathematical Society, 2001.
- [10] J. Cantarella, T. Needham, C. Shonkwiler, and G. Stewart. Random triangles and polygons in the plane. *The American Mathematical Monthly*, 126(2):113–134, 2019.
- [11] P. Chaudhuri and J. S. Marron. Scale space view of curve estimation. *Ann. Statist.*, 28:408–428, 2000.
- [12] R. R. Coifman and S. Lafon. Diffusion maps. *Appl. Comput. Harmon. Anal.*, 21(1):5–30, 2006.
- [13] J. Curry, H. Hang, W. Mio, T. Needham, and O. B. Okutan. Decorated merge trees for persistent topology. *J Appl. and Comput. Topology*, 6(3):371–428, 2022.
- [14] J. Curry, W. Mio, T. Needham, O. B. Okutan, and F. Russold. Stability and approximations for decorated Reeb spaces. In *Symposium on Computational Geometry*, Athens, Greece, June 2024.
- [15] D. H. Diaz Martinez, C. H. Lee, P. T. Kim, and W. Mio. Probing the geometry of data with diffusion Fréchet functions. *Appl. Comput. Harmon. Anal.*, 47(3):935–947, 2019.
- [16] A. Edelman, T. A. Arias, and S. T. Smith. The geometry of algorithms with orthogonality constraints. *SIAM journal on Matrix Analysis and Applications*, 20(2):303–353, 1998.
- [17] R. Flamary, N. Courty, A. Gramfort, M. Z. Alaya, A. Boissunon, S. Chambon, L. Chapel, A. Corenflos, K. Fatras, N. Fournier, et al. Pot: Python optimal transport. *Journal of Machine Learning Research*, 22(78):1–8, 2021.
- [18] M. Fréchet. Les éléments aléatoires de nature quelconque dans un espace distancié. *Ann. Inst. H. Poincaré*, 10:215–310, 1948.
- [19] E. Gasparovic, E. Munch, S. Oudot, K. Turner, B. Wang, and Y. Wang. Intrinsic interleaving distance for merge trees. *La Matematica*, 4(1):40–65, 2025.
- [20] K. Grove and H. Karcher. How to conjugate C^1 -close group actions. *Math. Z.*, 132:11–20, 1973.
- [21] K. Grove, H. Karcher, and E. A. Ruh. Group actions and curvature. *Invent. Math.*, 23:31–48, 1974.
- [22] K. Grove, H. Karcher, and E. A. Ruh. Jacobi fields and Finsler metrics on compact Lie groups with an application to differentiable pinching problems. *Math. Ann.*, 211:7–21, 1974.
- [23] H. Hang, F. Mémoli, and W. Mio. A topological study of functional data and Fréchet functions of metric measure spaces. *J Appl. and Comput. Topology*, 3(4):359–380, 2019.
- [24] J.-C. Hausmann and A. Knutson. Polygon spaces and grassmannians. *L’Enseignement Mathématique*, 43, 1997.
- [25] S. Hundrieser, B. Eltzner, and S. Huckemann. A lower bound for estimating Fréchet means. arXiv:2402.12290, 2024.
- [26] H. Karcher. Riemannian center of mass and mollifier smoothing. *Comm. Pure Appl. Math.*, 30:509–541, 1977.

- [27] A. Kasue and H. Kumura. Spectral convergence of Riemannian manifolds. *Tohoku Math. J.*, 46(2):147–179, 1994.
- [28] Y.-H. Kim and B. Pass. Wasserstein barycenters over Riemannian manifolds. *Adv. Math.*, 307:640–683, 2017.
- [29] H. Le. Locating Fréchet means with application to shape spaces. *Adv. Appl. Prob.*, 33:324–338, 2001.
- [30] T. Lindeberg. *Scale Space Theory in Computer Vision*. Kluwer, Boston, 1994.
- [31] F. Mémoli. On the use of Gromov-Hausdorff distances for shape comparison. In *Proceedings Point Based Graphics*, pages 81–90, 01 2007.
- [32] F. Mémoli. Gromov-Wasserstein distances and the metric approach to object matching. *Found. Comput. Math.*, 11(4):417–487, 2011.
- [33] D. Morozov, K. Beketayev, and G. Weber. Interleaving distance between merge trees. *Discrete Comput. Geom.*, 49:22–45, 2013.
- [34] R. R. Sokal and F. J. Rohlf. The comparison of dendrograms by objective methods. *Taxon*, 11:33–40, 1962.
- [35] K.-T. Sturm. On the geometry of metric measure spaces. *Acta Mathematica*, 196(1):65–131, 2006.
- [36] T. Vayer, L. Chapel, R. Flamary, R. Tavenard, and N. Courty. Fused Gromov-Wasserstein distance for structured objects. *Algorithms*, 13(9):212, 2020.
- [37] C. Villani. *Optimal Transport: Old and New*, volume 338. Springer Science & Business Media, 2008.
- [38] J. Weed and F. Bach. Sharp asymptotic and finite-sample rates of convergence of empirical measures in Wasserstein distance. *Bernoulli*, 25(4A):2620–2648, 2019.